Giri Jitender (Orcid ID: 0000-0001-6969-5187)
Chauhan Harsh (Orcid ID: 0000-0002-1396-5464)

PRpnp, a novel dual activity PNP family protein improves plant vigor and confers multiple stress tolerance in *Citrus aurantifolia*

Sweta Singh[1], Chanderkant Chaudhary[1], Rushikesh D. Bharsakale[2], Snehi Gazal[3], Lokesh Verma[4], Zeba Tarannum[1], G.T. Behere[2], Jitender Giri[4], Hugo Germain[3], Dilip K Ghosh[2], Ashwani K Sharma[1], and Harsh Chauhan[1*]

1= Department of Biosciences and Bioengineering, Indian Institute of Technology Roorkee, Roorkee, Uttarakhand, India 247 667

2= ICAR-Central Citrus Research Institute, Nagpur, Maharashtra, India 440 033

3= Department of Chemistry, Biochemistry and Physics, Université du Québec à Trois-Rivières, 3351 Bd des Forges, Trois-Rivières, QC G8Z 4M3, Canada

4= National Institute of Plant Genome Research, Aruna Asaf Ali Marg, New Delhi, India110 067

*= author for correspondence

ORCID: 0000-0002-1396-5464

Email: harsh.chauhan@bt.iitr.ac.in

Phone: +91 1332 284814

Keywords: *Putranjiva roxburghii* purine nucleoside phosphorylase (*PRpnp*), *Citrus aurantifolia*, abscisic acid (ABA), jasmonic acid (JA), cytokinin (CK) interconversion, plant defense

Summary

Under field conditions, plants are often simultaneously exposed to several abiotic and biotic stresses resulting in significant reductions in growth and yield; thus, developing a multi-stress tolerant variety is imperative. Previously, we reported the neofunctionalization of a novel PNP family protein, *Putranjiva roxburghii* purine nucleoside phosphorylase (PRpnp) to trypsin inhibitor to cater to the needs of plant defense. However, to date, no study has revealed the potential role and mechanism of either member of this protein group in plant defense. Here, we overexpressed *PRpnp* in *Citrus aurantifolia* which showed nuclear-cytoplasmic localization, where it functions in maintaining the intracellular purine reservoir. Overexpression of *PRpnp* significantly enhanced tolerance to salt, oxidative stress, alkaline pH, drought, and two pests, *Papilio demoleus* and *Scirtothrips citri* in transgenic plants. Global gene expression studies revealed that *PRpnp* overexpression up-regulated differentially expressed genes (DEGs) related to ABA- and JA- biosynthesis and signaling, plant defense, growth, and development. LC-MS/MS analysis validated higher endogenous ABA and JA accumulation in transgenic plants. Taken together, our results suggest that *PRpnp* functions by enhancing the endogenous ABA and JA, which interact synergistically and it also inhibits trypsin proteases in the insect gut. Also, like other purine salvage genes, *PRpnp* also regulates CK metabolism and increases the levels of CK-free bases in transgenic Mexican lime. We also suggest that *PRpnp* can be used as a potential candidate to develop new varieties with improved plant vigor and enhanced multiple stress resistance.

Introduction

Being sessile organisms, plants are constantly confronted by several abiotic and biotic stresses. Over the course of evolution, plants have developed complex defense machinery that produces numerous defensive proteins in response to adverse conditions. One such group of proteins comprises wound-inducible (WI) and vegetative storage proteins (VSPs). VSPs are found in all plant species and are primarily known to serve as nitrogen reserves in vegetative tissues. VSPs also possess sequence homology with pathogenesis-related proteins such as abscisic acid (ABA) and jasmonic acid (JA) responsive proteins (Tegeder and Masclaux-Daubresse, 2018). The defensive role of several WI proteins and VSPs have been reported, such as a sugarcane WI protein '*SUGERWIN2'* showed antipathogenic properties (Medeiros et al., 2012), JA-induced *Arabidopsis* VSP, *AtVSP2* exerts insecticidal activity against coleopteran and dipteran insects (Liu et al., 2005), and recently, a VSP, maize mesophyll lipoxygenase *ZmLOX6*, improved plant drought tolerance upon its overexpression (Abbaraju et al., 2022). However, the defensive role of several other similar proteins remained largely unknown (Verma et al., 2017).

Our research group was the first to identify and characterize a ~34 KDa *Putranjiva roxburghii* purine nucleoside phosphorylase (PRpnp) protein, isolated from the seeds of *P. roxburghii*, a medicinal plant belonging to the *Euphorbiaceae* family. Initially, PRpnp was reported as *P. roxburghii* trypsin inhibitor (PRTI) due to its nature as a competitive inhibitor of trypsin (Chaudhary et al., 2008). Later, we performed a detailed sequence analysis of *PRpnp* and reported the existence of a group of similar proteins that displayed sequence homology and evolutionary linkage to stress-induced proteins characterized as WI protein, VSPs, and bark storage proteins (BSPs). All the group members contain a purine nucleoside phosphorylase-uridine phosphorylase (PNP-UDP) family domain, disrupted with a stretch of amino acids. PRpnp showed an insertion of 46-amino acid residues in its PNP-UDP domain, which is responsible for its trypsin inhibitory nature and, thus, it possesses dual activity, i.e., PNP and protease (trypsin) inhibitory activity. The insertion of trypsin inhibitory loop is the case of neofunctionalization of PRpnp to a potent trypsin inhibitor (TI) to cater to the needs of plant defense (Verma et al., 2017; Verma et al., 2022).

Purine nucleoside phosphorylase (PNP; E.C.- 2.4.2.1), a salvage pathway enzyme of purine biosynthesis that catalyzes a reversible reaction to produce free purine base and (2′-deoxy)

ribose-1-phosphate (Verma et al., 2017). Purine nucleotides are the building blocks of nucleic acids, energy carriers, and cell signaling molecules and also play fundamental roles in metabolism (Zhao et al., 2015a). Purine salvage enzymes, including PNPs, are also involved in cytokinin (CK) metabolism (Ashihara et al., 2018). Stress conditions such as wounding require an abundant supply of adenine nucleotides; thus, the level of purine nucleotides and relative expression intensity of purine salvage genes and their *in vitro* activities over *de novo* were increased in wounded potato tuber slices (Katahira and Ashihara, 2006).

Protease inhibitors (PIs) are natural plant defense proteins that form stable protease-inhibitor complexes with their target proteases, thereby inhibiting them (Srinivasan et al., 2009). The defensive role of several PIs, including TIs, in response to both abiotic and biotic stresses, is widely known (Srinivasan and Kirti, 2012). Numerous transgenic plants overexpressing different PIs have been produced with enhanced stress tolerance (Srinivasan and Kirti, 2012; Clemente et al., 2019). The recurrent stress challenges in plants have pushed them to develop an efficient and resilient defense system. To accomplish this, numerous structural and functional changes in plant proteins have been observed during the course of evolution (Bartlett and Whipple, 2013). Similarly, PRpnp and other homologous proteins evolved and attained a disruption in the PNP-UDP domain (Verma et al., 2017; Verma et al., 2022). The purine salvaging capacity and neofunctionalization of PRpnp to trypsin inhibitor, along with its evolutionary linkage to other plant defense proteins, prompted us to explore its defensive role against multiple environmental stresses.

Citrus is one of the major fruit crops, grown in the tropical and subtropical regions of more than 140 countries and includes many species of economic importance, such as limes, oranges, lemons, grapefruit, and tangerines (Liu et al., 2012). Among the three classes of limes, *Citrus aurantifolia* is the globally predominant natural hybrid, with India, China, and Mexico as its prime producers; however, its cultivation is remarkably limited by numerous abiotic and biotic stresses (Donkersley et al., 2018). Under field conditions, *C. aurantifolia* experiences several stresses simultaneously, which hampers its growth and decreases the economic yield; therefore, developing a multi-stress tolerant variety is imperative. In this study, PRpnp showed nuclear-cytoplasmic localization and was constitutively overexpressed in Mexican lime. Transgenic plants showed enhanced tolerance to salt, oxidative stress, alkaline pH, drought, and two pests, *Papilio demoleus* and *Scirtothrips citri*. Furthermore, we found that *PRpnp* functions by enhancing the endogenous ABA and JA, which interact synergistically and it also inhibits trypsin proteases in the insect gut. Other important

functions of *PRpnp* include the maintenance of intracellular purine reservoir and CK homeostasis.

Results

PRpnp localizes to the nucleus and cytosol

The apparent molecular weight (MW) of PRpnp protein is ~34 kDa and pI value corresponds to 5.44. The modular structure of PRpnp protein is illustrated (Figure 1- a). The subcellular localization and functionality of a protein are likely interconnected (Yu et al., 2006). To examine the subcellular localization of PRpnp, we transiently expressed PRpnp-GFP fusion protein in *Nicotiana benthamiana* leaves. Upon 2 days post infiltration (dpi), laser-scanning confocal microscopy detected the green fluorescent signal of PRpnp-GFP protein in both the nucleus and cytosol (Figure 1- b: IV). The RFP was used as nucleocytoplasmic marker (Figure 1- b: II) and the nuclei were stained with 4',6-diamidino-2-phenylindole (DAPI) (Figure 1- b: III). The experiment was repeated thrice and showed the same subcellular localization for PRpnp (Figure 1- b).

Generation and confirmation of transgenic *C. aurantifolia* Cv. Pramalini

To end the speculation regarding its defensive role, *PRpnp* was chosen as an overexpression target, and the *Agrobacterium*-mediated transformation method was used to transform *C. aurantifolia* Cv. Pramalini, First, we successfully assembled the expression cassette in pBSSK(+) (Figure S1- a) and subsequently subcloned it to the binary vector pCAMBIA2301 (Figure S1- b-c). Putative transgenic shoots with kanamycin resistance and positive GUS histochemical activity were obtained. We observed no GUS activity in control. Finally, to recover the whole transgenic plant, the putative transgenic shoots were either *in-vitro* micrografted or cultured on rooting media. The stages of transgenic Mexican lime development are depicted (Figure S2).

To select the plants for subsequent experiments, we characterized the putative transgenic plants by duplex PCR (Figure S3- a) and quantitative real-time PCR (qRT-PCR) (Figure S3- b), which showed successful *PRpnp* gene integration and expression, respectively. Further, we detected bands corresponding to the expected MW of PRpnp protein, i.e., ~34 kDa, which marked its expression in transgenic plants by Western blot analysis. No equivalent band was detected in WT (Figure S4- a). Based on the results of qRT-PCR and Western blot analysis, transgenic plants that showed decent *PRpnp* expression and protein accumulation were chosen for further experiments in this study. All the GUS positive transgenic Mexican

limes that were developed in this study and their recovery method are documented (Table S1).

The total leaf protein fractions (200 µg) from WT and transgenic plants were isolated to assess PNP and trypsin inhibitory activity. To confirm the presence of PNP activity, we subjected the protein isolates to react with inosine and measured OD at 293 nm. We recorded a comparative increase in absorptions in the reaction mixture of transgenic plants A2, A6, and A11, which were, respectively, 3.6-, 1.95-, and 1.64 times higher than WT (Figure S4- b: I). Trypsin inhibitory activity was measured as percentage inhibition of trypsin (I%). Previous report quantifying I% from the protein fraction of transgenic plants is also available (Senthilkumar et al., 2010). Transgenic plants A2, A6, and A11, showed 68.41%, 56.54%, and 48.41 % inhibition percentages, respectively (Figure S4- b: II). The presence of both PNP and trypsin inhibitory activity confirms that PRpnp functions appropriately in transgenic *C. aurantifolia*.

Leaf disc senescence assay of transgenic *C. aurantifolia* shows tolerance to multiple abiotic stresses

Six transgenic plants A2, A6, A11, A28, A30, and A32, with variable *PRpnp* expression levels, were selected for leaf disc senescence assay. Leaf discs from healthy and fully expanded leaves of WT and transgenic plants were exposed to different stress solutions (200 mM and 300 mM NaCl for salt stress; 48 h and 72 h, 50 mM H_2O_2 for oxidative stress; 48 h, and pH= 9 for alkaline stress; 120 h) and was compared to control. The leaf discs of WT showed partial or complete bleaching depending upon the type/duration of stress applied; however, under the same conditions, no or significantly less bleaching was noticed in transgenic leaf discs. All the leaf discs remained green under control conditions (Figure 2- a-c). *PRpnp* overexpressing transgenic plants showed a clear advantage in overcoming the deleterious effect of NaCl, H_2O_2, and high pH. Further, biochemical investigations to evaluate the degree of stress-triggered cellular damage, the chlorophyll (a and b) and carotenoid were estimated. After imposing the stresses, we noticed significantly higher pigment retention in all the transgenic plants over WT. Furthermore, among all the transgenic, plant A2 showed the highest, whereas A28 showed the lowest retention of tested pigments under all the stress conditions (Figure 2- d-f). Under salt stress (300 mM; 72 h), oxidative stress, and alkaline stress, transgenic plants A2 could retain 2.3-, 3.3-, and 1.99 times; 1.99-, 2.24-, and 1.70 times; 2.48-, 2.79-, and 2.08 times while plant A28 showed 1.48-, 2.25-, and 1.39 times; 1.35-, 1.25-, and 1.11 times; 1.29-, 1.38-, and 1.22 times higher

Chlorophyll a (chl a), Chlorophyll b (chl b), and carotenoids content, respectively over WT (Figure 2- d-f). Overall, these results documented the usefulness of *PRpnp* overexpression in providing multiple stress resistance in transgenic plants.

Overexpression of *PRpnp* improves tolerance to high salt concentration also at the whole plant level

Generally, leaf disc senescence assay involves using a higher concentration of NaCl to see the results in a shorter period. Thus, it does not reflect the actual tolerance limits of transgenic plants under natural conditions (Bhaskaran and Savithramma, 2011). Therefore, to further validate the stress-responsive role of *PRpnp* at the whole plant level, we treated WT and selected transgenic *C. aurantifolia* A17, A19, and A21 with 75 mM NaCl for 45 days. Since we harvested leaves from WT and transgenic plants for leaf disc senescence and other detached leaf assays (described in later sections), and due to the long juvenile period in *C. aurantifolia*, we used different sets of plants to assess salt and drought tolerance at whole plant level. However, the expression of *PRpnp* transcript (Figure S3- b) and protein (Figure S4- a) in every plant was determined before proceeding. The plants selected for assessing salt and drought stress tolerance under soil conditions were recovered by rooting. Plants of similar age and height were selected for this study. Also, all the selected transgenic plants were clonally propagated to generate at least 4-6 identical plants using standard method of citrus node culture to perform three biologically independent experiments. From the third week of treatment, WT started showing severe salt stress-induced damage including leaf wilting that was simultaneously accompanied by leaf rolling, tip-initiated leaf burning, and leaf abscission which subsequently caused plant death. By contrast, no severe symptoms were detected in transgenic plants (Figure 3- a). Moreover, the physiological parameters including proline and malondialdehyde (MDA), were estimated in WT and transgenic plants at 0 days, 25th day, 40th day, and 45th day. Being a compatible osmolyte and reactive oxygen species (ROS) scavenger, increased proline levels have been widely proven to play a crucial role in salt and drought tolerance (Kavi kishor and Sreenivasulu, 2014). The strength of plant responses to adverse environmental conditions is marked by MDA, an indicator of lipid peroxidation of cell membranes (Song et al., 2022). Thus, increased MDA levels could be determinantal to plants. The same-day comparison showed that the significant increase in proline was higher, and MDA was lower in transgenic plants relative to WT plants. No significant differences were observed at day 0. Proline accumulation in *PRpnp* overexpressing plants A17, A19, and A21 showed 136.68, 112.97, and 82.30 percent increase

(%) (Figure 3- b) while percent decrease (%) in MDA levels were 57.76, 41.84, and 43.47 (Figure 3- c) relative to WT, at 45th day of salt stress treatment. With no significant sign of salt-elicited leaf damage, high proline content, and low MDA levels, the results show that transgenic plants are tolerant toward salt stress compared to WT. Thus, the overexpression of *PRpnp* significantly alleviated the deleterious effects of salt stress in transgenic *C. aurantifolia*.

Overexpression of *PRpnp* improves tolerance to drought

To examine the role of *PRpnp* in regulating drought stress tolerance, watering to WT and transgenic citrus, A22, A24, and A25 were withheld for 25 days. All the plants used in the study were cultivated under a fully watered regime before stress treatment. No phenotypic differences were observed among the plants in the first week of drought. However, by the second week, severe symptoms of water deficiency, such as light green and yellow-green foliage, leaf wilting, curling, and drying followed by twig dieback, were observed in WT, while transgenic plants showed no significant drought-induced symptoms. New foliage development in A22 and A24 during drought indicated superior growth and metabolism rates over WT. Normal watering conditions were resumed after 25 days in all the plants for stress recovery, and observations were made after 15 days. We observed poor recovery in WT upon rewatering; however, transgenic plants rejuvenated quickly (Figure 4- a). To combat the episodic drought or watering pulse, the plant usually abandons its older parts and produces new ones upon rewatering (Xu et al., 2010). We observed a similar pattern of drought stress survival in *PRpnp* transgenic plants during recovery (Figure 4- a). The phenotypes of WT plants which were in contrast to the performances of *PRpnp* overexpressing plants under the same stress conditions, supported the positive role of *PRpnp* in response to drought. This was further validated by quantification of proline, MDA, and relative water content (RWC). At the end of treatment, with 120.037%, 79.42%, and 94.35% increase in proline accumulation (Figure 4- b) and 56.06%, 40.17%, and 50.20% decrease in MDA levels (Figure 4- c), transgenic plants A22, A24, and A25, respectively, performed better in tolerating drought, compared to WT. Additionally, A22 maintained 50.83%, followed by 37.80% and 45.07% RWC in A24 and A25, while WT could only retain 22.25% (Figure 4- d). Together, these results indicate that *PRpnp* overexpression enhances drought tolerance in transgenic *C. aurantifolia* relative to WT.

Overexpression of *PRpnp* confers resistance to *P. demoleus* larvae

TIs are well known to confer resistance to Lepidopteran in transgenic plants (Srinivasan et al., 2009; Srinivasan and Kirti, 2012). Since PRpnp also possesses protease inhibitory activity, we hypothesized that it could promote pest resistance. To investigate this, leaves of three transgenic plants, A2, A6, and A11, were challenged to five-second instar larvae of *P. demoleus* and compared with the control. The visible comparative growth of WT-fed larvae was superior to transgenic ones (Figure 5- a-c). This was supported by the declined average body weights of A2, A6, and A11 fed larvae which were, respectively, 5.47-, 4.48-, and 3.25 times less than control at 12 day-post-hatching (12 DPH). Comparatively, transgenic-fed larvae gained significantly less body weight between 9 and 12 DPH; however, WT-fed larvae displayed normal growth rates (Figure 5- b-d). The declined body weights were directly related to reduced herbivory. At 12 DPH, 53 % larval mortality was recorded in A2, followed by A6 and A11 fed larvae which were, respectively, 46 %, and 26%, while no larval mortality was observed in the WT plant (Figure 5- e). From the results, it was apparent that overexpression of the *PRpnp* gene in *C. aurantifolia* plants improves resistance to *P. demoleus* larvae.

Overexpression of *PRpnp* promotes resistance to adult *S. citri*

We further extended our study by investigating the insecticidal properties of *PRpnp* against another pest, adult *S. citri*. To evaluate this, a detached leaf bioassay of WT and transgenic plants, A2, A6, and A11, was performed. Each leaf was infested with 18-20 thrips (Figure 6- a-b). The surviving thrips were counted manually, and their mortality was recorded every 24 h for 3 days. Few WT- and transgenic-fed thrips were imaged under the microscope after 72 h (Figure 6- c-d). The declining population of adult citrus thrips and increased corrected mortality (%); (CM %) were linked to the insecticidal effects of *PRpnp* overexpression in transgenic plants. The maximum recorded CM (%) after 72 h was 59.11, 53.17, and 40.52, respectively, for A2, A6, and A11 plants (Figure 6- e). Taken together, the reduced survival rates of adult citrus thrips upon transgenic plants, compared to control, confirmed the advantage of *PRpnp* overexpression in *C. aurantifolia*.

***De novo* transcriptome profiling analysis identified highly enriched GO terms and differentially expressed genes (DEGs) in WT and *PRpnp* transgenic *C. aurantifolia* under control conditions**

The multiple stress resistance phenotype of transgenic *C. aurantifolia* prompted us to investigate how overexpression of *PRpnp* affects the global gene expression profiles. To accomplish this, we performed high-throughput RNA-seq experiments on WT and transgenic

plants under control conditions. A total of ~52 million raw reads were generated, with approximately ~25 million and ~27 million high-quality reads for WT and transgenic plants, respectively. Out of 6348 identified DEGs, 3308 DEGs were up-regulated, and 3040 DEGs were down-regulated in WT and transgenic samples (Table S2). The principal component analysis (PCA) plot analysis validated the discrimination between the transcriptome profiles and showed that the WT samples were clustered together, and there was a significant sample-to-sample distance between WT and transgenic counterparts (Figure S5- a). Furthermore, we illustrated the distribution of up-regulated and down-regulated DEGs by volcano plot (Figure S5- b).

We performed GO enrichment analysis and functional annotation of DEGs by BiNGO in Cytoscape software (Figure S6). The network analysis showed that GO of 'response to hormone stimulus', response to abiotic stimulus', 'response to biotic stimulus', 'cellular nitrogen compound metabolic process', 'anatomical structure development', 'embryonic development', 'root morphogenesis', 'transport', 'potassium ion transport', 'calcium ion transport', 'cell cycle', 'plastid organization', 'chloroplast organization', and 'ion homeostasis' were significantly enriched in the up-regulated DEGs (Figure S6- a-e) whereas GO terms belonging to 'anatomical structure morphogenesis', 'post-embryonic development', 'shoot morphogenesis', 'cell wall organization or biogenesis', and 'protein modification process' were enriched in the down-regulated DEGs (Figure S6- f-h).

The variation in the expression of selected DEGs is shown in the heat maps, and their relative expression levels are depicted in different colors (Figure S7). DEGs analysis suggested that the genes belonging to phytohormone biosynthesis and signaling (*AAO3*, *PYL9*, *LOX6, OPR3*, *4CLLs*, *ADK2*, *LOG2*), plant defense and transcription factors (TFs) (*PRXIIF, MES1, HSP90-5*, *HSFA4A*, *DTX35, APX1*, *BZIP60*, *BHLH130*, *NAC52*, *WRKY75*), cell cycle (*CDC6B*, *APC7*, *SPC25*), DNA repair (*PAXIP1*, *MLH3*, *DRT111*, *RAD50*, *LIG6*), transporters (*ABCG40*, *ABCB25*, *ABCC3*, *ECA3*, *HAK5*, *CAT5*), photosynthesis (*PHOT1B*, *LHCB4.3*, *CIB22*, *psaA*, *SOQ1*), development (*NFS2*, *CTL1*, *HPT1*, *HMGB9*, *RER1*), and metabolism (*SPS4*, *PFK3*, *HXK2*, *HIDM*) were significantly up-regulated (Figure S7- a-i). The down-regulated genes belong to categories such as lipid metabolism (*KCS2*, *HHT1*, *CYP86A2*, *FAR3*), cell fate (*LIS*, *YAB5*, *GL3*, *WER*), catabolism (*LAC11*, *PME8*, *XYL1*), and development (*COL9*, *EMF2*, *FIE2*, *CLF*). Genes that negatively regulate hormone signaling (*PP2C51*, *ICMTB*, *ARAC7*, *ATAF1*, *B'GAMMA*, *APT1*) were also down-regulated (Figure S7- j-m). Total up-regulated and down-regulated DEGs in *PRpnp* transgenic *C. aurantifolia* are

documented in Table S3 and S4, respectively. The global view of the transcriptomic data showed that even without stress signals, the expression of genes associated with plant defense, growth, and development was significantly up-regulated in transgenic plants, suggesting the reason for being more resilient to adverse environmental conditions over WT.

LC/MS-MS analysis validates higher accumulation of endogenous ABA, JA, and CK in *PRpnp* transgenic plants

After analyzing the transcriptome data, we realized that the genes related to ABA and JA biosynthesis and signaling pathways had been up-regulated. Also, some previous work has claimed the participation of purine metabolism enzymes in CK metabolism (Schoor et al., 2011; Zhang et al., 2013). Since *PRpnp* is a salvage pathway enzyme of purine biosynthesis (Verma et al., 2017; Verma et al., 2022). Thus, we anticipated the role of *PRpnp* in catalyzing CK interconversion reactions. To understand the phytohormonal regulation by overexpression of *PRpnp* in *C. aurantifolia*, we performed a targeted profiling of ABA, JA, and CK in WT and transgenic plants by LC-MS/MS under normal growth conditions. Consistent with our transcriptome data and hypothesis, phytohormone quantification revealed that *PRpnp* transgenic *C. aurantifolia* had a substantially higher accumulation of ABA (~1.86-fold), JA (~2.56-fold), and CK-free base tZ (~2.1-fold), compared to WT. The concentration (ng g^{-1} FW) in transgenic plants was estimated to be 41.90, 148.73, and 1.05, whereas the concentration in WT was 22.50, 58.67, and 0.48, respectively, for ABA, JA, and CK (Figure 7- a-c). It seems that *PRpnp* could elevate the expression of ABA and JA related genes thus, promotes their co-accumulation and synergistic interaction. *PRpnp* could also be involved in CK metabolism by regulating its interconversion and promoting the accumulation of CK-free bases.

Discussion

Plants are the fundamental pillars for sustaining a balanced ecosystem for all life forms; thus, advanced sequencing techniques frequently upgrade the plant genome and proteome databases. However, the roles of several plant genes and proteins remain undiscovered. Similarly, one “yet to be studied” group of proteins is related to WI protein and VSPs and shows homology to nucleoside phosphorylases. In our previous studies, we characterized one of the proteins from this group i.e., PRpnp and proved its neofunctionalization to a trypsin inhibitor (Chaudhary et al., 2008; Verma et al., 2017; Verma et al., 2022). We speculated *PRpnp* as a potential candidate that can promote multiple stress tolerance in plants. Since it is a purine salvage enzyme and no other studies have shown the defensive role of *PRpnp* or

other members of this protein group. Thus, we have overexpressed *PRpnp* in *C. aurantifolia* to extend our knowledge and understanding of the importance of this novel PNP family protein.

We determined the subcellular localization of PRpnp to decode its function. In this study, PRpnp was co-localized in the nucleus and cytosol upon transient expression of PRpnp-GFP fusion protein in *N. benthamiana* by agro-infiltration (Figure 1- b). Previously, few studies unveiling the localization of mammalian PNPs have been documented; although, to our best knowledge, no such reports on plant PNPs are available. The reported PNPs are cytosolic enzymes (Rubio and Berne, 1980; Giuliani et al., 2017), though nuclear-cytoplasmic (Castellano et al., 1990), mitochondrial (Haag and Lewis, 1994), and extracellular PNPs (Giuliani et al., 2017) are also present. As purine nucleotides are crucial for nucleic acid generation, providing cellular energy (ATP), intracellular signaling (GTP), and also serve as cofactors such as NAD and coenzyme A (Pedley and Benkovic, 2017), thus all the dividing, differentiating, and fully differentiated cells seek a vast supply of purines throughout life (Giuliani et al., 2017). Inside the cell, purine nucleotides control G_1 to S phase transition and progression through the S phase (Quéméneur et al., 2003). In a study, the growth rate of cultured fibroblasts increased upon increasing the supply of purine nucleotides due to the promotion of the G1/S transition and ATP production (Kondo et al., 2000). Purine metabolites are also involved in DNA repair by promoting the repair of the double-strand breaks (DSBs) (Zhou et al., 2020). Consistent with these findings, the nuclear-cytoplasmic localization of PRpnp corroborates that it could regulate several biological processes in the nucleus and cytosol by maintaining the intracellular purine reservoir. *PRpnp* could also promote nucleic acid synthesis, DNA replication, and even DNA repair by fulfilling the need of purine nucleotides in the nucleus. However, the mechanism of nuclear transport of PNPs remained unclear.

After abiotic stress treatment, *PRpnp* transgenic plants showed significantly higher retention of chl a, chl b, and carotenoids in leaf disc senescence assays that signifies their enhanced tolerance against salt, oxidative and alkaline pH stress, compared to WT (Figure 2). Previous reports are available showing the reduction in the concentration of chlorophyll and carotenoid under the influence of several stresses (Sidhu et al., 2017; Hamani et al., 2020). Further, *PRpnp* overexpressing plants also showed salt tolerance under soil conditions (Figure 3) and drought tolerance (Figure 4). To reveal the underlying mechanism that leads to multiple stress tolerance in Mexican lime by overexpressing *PRpnp*, we performed *de novo* transcriptome

profiling of WT and transgenic plants, under normal growth conditions. We found a comprehensive set of genes involved in phytohormones majorly, ABA and JA biosynthesis and signaling, plant defense, cell cycle, DNA repair, TFs, transporters, development, and metabolism were up-regulated in transgenic plants (Figure S7).

Phytohormones are the steward of plant defense and responses. They coordinate the environmental signals with developmental processes and are the basis of stress endurance in plants (Altmann et al., 2020). Several essential genes related to ABA such as biosynthesis (*AAO3*), cofactor (*ABA3*), TFs (*ABF2*, *BZIP16*, *BZIP60*, *BHLH130*, *NAC52*), other positive regulators (*ARIA*), ABA importers (*ABCG40*), receptors (*PYL9*) were differentially up-regulated (Figure S7- a, c, d). Moreover, a negative regulator of ABA-mediated responses, protein phosphatase 2C clade A member (*PP2C51*), was differentially down-regulated in *PRpnp* transgenic plants (Figure S7- j). Similarly, JA biosynthesis (*LOX6*, *OPR3*, *AOC3*, *4CLL5*, *4CLL7*, *4CLL9*, *KAT2*) and positive regulators (*WRKY75*, *PLA1*) were also up-regulated in transgenic plants (Figure S7- a, c). Previous studies have elucidated the importance of these genes in phytohormone mediated signaling and their role in improving stress resistance in plants (Table 1 and 2). Through the transcriptome data, we anticipated that even without stress signals, *PRpnp* transgenic plants could accumulate higher levels of endogenous ABA and JA, relative to WT plants. Our LC-MS/MS data confirmed this and quantified higher levels of both phytohormones in transgenic plants (Figure 7).

Literature is available that shows, under natural conditions, plants protect themselves by elevating endogenous ABA (Vishwakarma et al., 2017) and JA (Kim et al., 2021) which in turn increases transcript levels of WI protein (Moura and Ryan, 2001) or VSPs (Avice et al., 2003) or TIs (Srinivasan et al., 2009), indicating their prominent role in plant stress tolerance. In agreement with this, overexpression of WI proteins (Medeiros et al., 2012), VSPs, (Abbaraju et al., 2022), and TIs (Srinivasan et al., 2009) enhances abiotic and biotic stress tolerance; however, the mechanism behind improved stress resistance in transgenic plants are still unknown. In our study, we found that upon overexpression, *PRpnp* elevated the endogenous accumulation of ABA and JA which is responsible for the resistant phenotypes in Mexican lime. This suggests that *PRpnp* overexpression might be involved in some regulatory mechanism or produce signals that trigger the transgenic Mexican lime to produce "stress fighting" phytohormones more than the usual level. From this, we can conclude that, when overexpressed, other similar proteins such as WI protein, VSPs, or TIs could also increase the basal levels of defense hormones such as ABA or JA which enhances stress

resilience in plants. The elevated phytohormone in turn could increase the expression of WI proteins, VSPs, TIs, and other stress-responsive genes. Additionally, over time, *PRpnp* evolved and attained an additional trypsin inhibitory property. The fundamental function of TIs is to prevent the degradation of the total protein content of the cell by blocking the proteases (Srinivasan et al., 2009; Srinivasan and Kirti, 2012). It seems that under natural stress conditions, *PRpnp* might be involved in the suppression of proteases that would improve the stability of various stress-responsive proteins and enhances basal plant immunity. Thus, *PRpnp* transgenic plants must be superior to WT in having a ceaseless and undegraded protein pool. Collectively, *PRpnp* not only elevates ABA and JA levels but also improves the survival of other stress-responsive proteins thus, improves plant vigor and stress resistance in transgenic plants.

From the parallel accumulation of ABA and JA we conclude that upon stress perception, both the signaling pathways would work synergistically, complementing each other responses including other metabolic and signaling pathways in response to abiotic stresses in transgenic *C. aurantifolia*. Evidences showing the existence of synergism between ABA and JA in the regulation of the plant response to abiotic and biotic stress are available (de Ollas et al., 2015; Kim et al., 2021; Li et al., 2022). Moreover, the increased proline accumulation and RWC (Figure 3- b, 4- b, d) and decreased MDA levels (Figure 3- c, 4- c) in transgenic *C. aurantifolia* upon stress treatments, relative to WT are consistent with previous reports that show similar results (Cui et al., 2011; Ma et al., 2020). Therefore, the increased proline and RWC may have shielded the antioxidative enzymes and excess water loss, respectively and low MDA levels prevented membrane damage in transgenic Mexican lime thus, alleviating the deleterious impacts of salt and drought stress.

The improved plant vigor of *PRpnp* transgenic plants was evident by upregulation of several important plant defense and TFs genes/families that protect plants from stresses and majorly belong to peroxiredoxins, heat shock protein, and heat stress TFs, L-ascorbate peroxidases, cysteine-rich receptor-like kinases (CRKs), G-type lectin S-receptor-like serine/threonine protein kinase (GsSRK), bZIP and WRKY family (Figure S7- b, c). In agreement with the studies that reveal the importance of purine nucleotides in G_1 to S phase transition (Quéméneur et al., 2003), progression through the S phase (Kondo et al., 2000), and DNA repair (Zhou et al., 2020), our transcriptome data, showed the up-regulation of a number of gene sets that positively regulates cell cycle and DNA repair in *PRpnp* transgenic plants (Figure S7- e-f). We also found multiple gene sets involved in photosynthesis, especially

those related to photosynthetic electron transport such as photosystem II (PSII), photosystem I (PSI), and ATP synthase were up-regulated in transgenic plants (Figure S7- g). This highly intact photosynthetic machinery suggests that it could be one of the major factors leading to higher pigment retention in transgenic plants during leaf disc senescence assay.

PIs such as TIs are shown to significantly impair the growth of Lepidopteran larvae (Srinivasan et al., 2009). Intake of TI along with food inhibits nutrient absorption and produces a feed inhibition signal which ultimately causes insect death (Zhao et al., 2019). Therefore, *PRpnp* was expected to improve insect resistance. Consistently, the feeding assay conducted with *P. demoleus* larvae showed significantly decreased body weights and increased mortality rates of transgenic-fed larvae in comparison to the control (Figure 5- d-e). This caused due to the inhibition of digestive proteases of *P. demoleus* larvae, which is majorly trypsin. The inhibited proteolytic process by PRpnp led to the unavailability of essential amino acids and caused physiological stress followed by retarded insect growth and death.

The proteolytic activity in the whole extracts of *Frankliniella occidentalis*, a thrips that belongs to the same family as of *S. citri* is predominantly cysteine proteases (Annadana et al., 2002). Later, Kuipers and Jongsma, (2004) also reported cysteine proteases as prime digestive enzymes in thrips gut. Though *PRpnp* is a trypsin protease inhibitor, we apprehended that it might not have a direct role in thrips resistance. However, in several previous reports, JA restricted thrips performance and preference, and also improved resistance (Abe et al., 2008; Abe et al., 2009). A dramatic increase in thrips attraction was observed in non-infected JA-insensitive *coi1-1* mutants compared with WT plants (Abe et al., 2009). Exogenous application of methyl jasmonate restored the thrips repellency effect in tomato mutants *def-1* which was impaired in JA biosynthesis (Escobar-Bravo et al., 2017). We also found increased mortality in transgenic-fed adult *S. citri*, compared to control (Figure 6- d). From this, we conclude that the increased JA levels due to *PRpnp* overexpression in Mexican lime enhanced thrips resistance.

Naturally occurring CKs are N^6 derivatives of adenine (Frebort et al., 2011). Among all the cytokinin metabolic processes, its interconversion plays a pivotal role in maintaining CK homeostasis. The purine salvage enzymes are known to catalyze the interconversions of CK bases, ribosides, and nucleotides (Ashihara et al., 2018). So, we anticipated *PRpnp*, an enzyme of purine salvage pathway could be involved in CK metabolism. We detected a

higher level of endogenous CK-free base; tZ in *PRpnp* transgenic plants by LC-MS/MS (Figure 7- c). Thus, *PRpnp* plays an important role in promoting CK interconversions, positively regulating the level of active CK bases, and thus maintaining its homeostasis.

Collectively, in this study, we constitutively overexpressed PRpnp, a novel PNP family protein in *C. aurantifolia* Cv. Pramilini and obtained transgenic plants with enhanced tolerance to various abiotic and biotic stresses. Moreover, our results indicated the mechanism by which overexpression of *PRpnp* enhanced stress tolerance in transgenic Mexican lime that involves increasing the endogenous levels of ABA and JA and promoting their synergistic interactions. We also found other important functions of PRpnp including the maintenance of intracellular purine reservoir, CK homeostasis, and improving plant vigor.

Experimental procedures

Subcellular localization of PRpnp

For subcellular localization, *PRpnp-GFP* fusion cassette was made under the control of the constitutive CaMV 35S promoter (35S::PRpnp-GFP). *PRpnp* gene was amplified without stop codon and cloned into the entry vector, pDONR221. The entry clone was then shuttled to the destination vector pB7FWG2 by Gateway technology (Karimi et al., 2002). Overnight grown *Agrobacterium* strain GV3101 harboring pB7FWG2-35S::PRpnp-GFP vector was infiltrated into the abaxial surface of 4-week-old leaves of *N. benthamiana*. For constitutive expression of RFP, vector pK7WG2-RFP was infiltrated. Live-cell imaging using laser scanning confocal microscopy was performed with a Leica TCS SP8 (Leica Microsystems, Wetzlar, Germany) and the images were processed with software LAS-AF (Version 4.0.0.11706).

Construction of overexpression vector

For generating the *PRpnp* overexpression construct, CaMV 35S promoter (enhanced), *PRpnp* (Accession number: HQ332518), and T-nos were assembled in pBSSK(+) and then subcloned into binary vector pCAMBIA2301 to generate the pCAMBIA2301-2x35S::PRpnp construct. Hypervirulent *Agrobacterium* strain EHA105 was used for plant transformation. All the plasmids used in the study were confirmed by sequencing before proceeding. The primers and PCR conditions are documented in Table S5 and S6, respectively.

Plant material preparation

Sterilized mature seeds of *C. aurantifolia* Cv. Pramalini were germinated on SG media for 3-4 weeks at 25±2 °C in dark, followed by one week under a 16-h photoperiod. Light green epicotyls of ~2 cm^2 length with oblique cut ends were pre-treated in 60 ml of LM2NB media for ~3-4 h and used for transformation.

***Agrobacterium*-mediated transformation and regeneration**

Agrobacterium strain EHA105 harboring binary vector pCAMBIA2301-2x35S::PRpnp was revived on YEM agar. One loop of the culture was inoculated to yield an OD_{600} of 0.3 into 60 ml of YEM broth on the day of transformation with appropriate antibiotics and 100 µM acetosyringone. The *Agrobacterium* cells were centrifuged and resuspended in MSA (OD_{600}= 0.3). The pre-treated epicotyls were infected by *Agrobacterium* for 15 min and blotted dry on sterile Whatman filter paper. Infected epicotyls were co-cultivated and regenerated, respectively on SMA2NB media for 2 days and MRNB1 media for 4 weeks at 25±2 °C in dark and later shifted to a 16-h photoperiod for one additional week.

Screening and hardening of putative transgenic plants

The basal portion of regenerated shoots was tested histochemically for GUS activity (Jefferson et al., 1987). Transgenic plants were recovered either by rooting or *in-vitro* micrografting. For rooting, the GUS positive shoots were cultured on MR media whereas, for *in-vitro* micrografting, the scion-rootstock system was cultured on ML media. GUS negative shoots were discarded. Recovered transgenic plants were slowly acclimated to the greenhouse conditions. All the media compositions are documented in Table S7.

Confirmation of putative transgenic plants

The total genomic DNA was isolated from the leaves of WT and putative transgenic plants using DNeasy® plant mini kit (69104; Qiagen, Hilden, Germany) according to the manufacturer's protocol and quantified with NanoDrop microvolume UV-Vis spectrophotometers (ND-ONE-W; Thermo Fisher Scientific, Waltham, USA). To confirm the stable transgenic plants, we performed duplex PCR and amplified *PRpnp* and *nptII* using the gene-specific primers and genomic DNA.

RNA extraction and transcript analysis

Leaves of WT and PCR-positive transgenic plants were used to extract the total RNA with RNeasy® plant mini kit (74904; Qiagen, Hilden, Germany) as per the manufacturer's instructions and was quantified. First-strand cDNA was synthesized (1708841; Bio-Rad, Hercules, USA), and qRT-PCR assay was performed in 96-well optical plates using SYBR

Green dye (A25741; Applied Biosystems™, Waltham, USA) and QuantStudio™ 5 real-time PCR system (A28574; Applied Biosystems™, Waltham, USA). QuantStudio™ Design and Analysis Desktop Software v1.5.1 was used for analysis. The expression of the *PRpnp* gene in transgenic plants was confirmed by comparing its cycle threshold (C_t) value with WT plants. The relative quantification of *PRpnp* gene was normalized to the cytochrome oxidase gene (*cox*) and calculation was done by comparative C_T method (Livak and Schmittgen, 2001).

Western blot analysis

The total leaf protein was isolated (Omar et al., 2007) and quantified (Bradford, 1976) as described previously and then transferred to PVDF membrane (IPVH00010 Immobilon®-P; MilliporeSigma™, Burlington, USA). After blocking, the membrane was first incubated with anti-PRpnp antibody (1:1000) followed by anti-rabbit IgG, HRP linked antibody (1:2000) (7074P2; Cell Signaling Technology, Danvers, USA). The protein blots were detected by Pierce™ ECL Western blotting substrate (32109; Thermo Fisher Scientific, Waltham, USA) as per the manufacturer's protocol using ChemiDoc™ (1708265; Bio-Rad, Hercules, USA).

Analysis of PNP and trypsin inhibitory activities

The total protein was isolated and tested for PNP (Verma et al., 2017) and trypsin inhibitory activity (Yao et al., 2001) as described earlier.

Leaf disc senescence assay for multiple abiotic stress resistance

The leaf discs of 1 cm diameter were excised from 18-20 months old plants. An equal number of leaf discs (n=12) were floated in 15 ml of ½ strength Hoagland solution supplemented with NaCl (200 mM and 300 mM; 48 h and 72 h) and H_2O_2 (50 mM; 48h) for salt and oxidative stress, respectively. For alkaline stress, leaf discs were dipped in 15 ml of ½ strength Hoagland solution of pH=9 for 120 h. An equal volume of ½ strength Hoagland solution (pH=5.8) without any supplements was used for the control experiment. Leaf discs were incubated at 25± 2 °C under continuous white light. Chlorophyll and carotenoids were quantified as already described (Hiscox and Israelstam, 1979).

Analysis of salt stress tolerance at the whole plant level

18-20 months old plants were irrigated twice a week for 45 days with an equal amount of ¼ strength Hoagland solution supplemented with 75 mM NaCl. To minimize the environmental variations, the positions of pots in the greenhouse were interchanged daily. The free proline and MDA content were estimated at regular intervals.

Analysis of drought stress tolerance

18-20 months old were assessed for drought stress tolerance. To evaluate the drought tolerance, water supply to plants was withheld for 25 days. The same environmental condition was given to every plant. Plants were photographed and proline levels, MDA content, and RWC estimations were done at different time points. After the drought stress period, the plants were reirrigated and evaluated for survival after 15 d.

Quantification of proline, MDA and RWC

The free proline content was calculated as described previously (Bates et al., 1973). Lipid peroxidation was estimated by quantifying the MDA level following the method described by Hodges et al, (1999). The MDA concentration produced in the sample was estimated by the equation described by Jha et al, (2013). RWC was estimated as already documented (Morgan, 1984).

Detached leaf bioassay for evaluating resistance to *P. demoleus* larvae

Tender leaves were fed to five second instar larvae of *P. demoleus*. The insects were kept at 25 °C under a 16- h photoperiod with 70 % relative humidity and larval body weight was recorded at regular intervals. The mortality rate of the larvae was calculated at 12 DPH using the formula described earlier (Zubair et al., 2019).

Detached leaf bioassay for evaluating resistance to adult *S. citri*

For detached leaf bioassay, young and tender leaves were wrapped in cotton and sealed with Parafilm. A small cut was made in the sealed portion to add water droplets periodically to prevent leaf drying. The thrips were cultured at 30 °C in a 16- h photoperiod. To determine the mortality rate, the *S. citri* were counted manually using a double-lens magnifying glass at different time points and imaged using a stereomicroscope (M205 A; Leica, Wetzlar, Germany). Mortality data were corrected by using Abbott's formula (Abbott, 1925).

Transcriptome profiling and analysis

Total RNA was isolated from WT leaves and *PRpnp* transgenic plants as described earlier and used for *de novo* transcriptome profiling. Two biological replicates were used for the analysis, and RNA-Sequencing was performed using the Illumina HiSeq platform with paired end read length of 101 bp at Bionivid Technology Private Limited (Bengaluru, India). NGSQC toolkit was utilized to check the quality (Phred score >20) of raw reads (https://github.com/mjain-lab/NGSQCToolkit, Patel and Jain, 2012). *De novo* assembly and mapping were performed using Trinity software

(https://github.com/trinityrnaseq/trinityrnaseq, Haas et al., 2013). The abundance estimation was calculated using RNA-Seq by Expectation-Maximization (RSEM) method (Li and Dewey, 2011). The differential gene expression analysis was performed using DESeq2 (https://bioconductor.org/packages/release/bioc/html/DESeq2.html, Love et al., 2014). Transcripts having log2 fold change greater ≥ than 2 were considered as differentially expressed genes (DEGs). The functional annotation of the transcriptome was performed using the Trinotate pipeline (https://github.com/Trinotate/Trinotate.github.io/blob/master/index.asciidoc), employing uniport-Swissprot (https://ftp.uniprot.org/pub/databases/uniprot/current_release/knowledgebase/complete/) database for blastx and blastp searches. Cytoscape (v 3.9.1) plug-in bingo was used to perform Gene Ontology (GO) enrichment and network analysis (Maere et al., 2005). Further, heat maps were constructed using gplots and RColorBrewer R packages (Warnes et al., 2022; https://CRAN.R-project.org/package=RColorBrewer, Neuwirth and Neuwirth, 2014). Principal component analysis (PCA) and volcano plots were constructed using python.

ABA and JA quantification

Briefly, around 200-250 mg of fresh tissues were grounded in liquid nitrogen. Methanol (1 ml) and internal standard (IS; 4 µl) were added to each sample followed by centrifugation. The samples were dried using SpeedVac concentrator (Savant SPD1010; Thermo Fisher Scientific, Waltham, USA). The methanol (400 µl) reconstituted samples were subjected to LC-MS/MS (QTRAP 6500+; SCIEX, Framingham, USA) for ABA and JA estimation.

CK quantification

Fresh plant tissue (200-250 mg) was grounded in liquid nitrogen and extracted in extraction buffer (1 ml; methanol: water: formic acid; 15:4:0.1) with 10 µl of IS. The sample was centrifuged and the collected supernatant was purified with C_{18} RP SPE column and eluted in 0.1% formic acid in acetonitrile. The samples were dried using SpeedVac concentrator and reconstituted in 100 µL of 5% methanol and subjected to LC-MS/MS.

Statistical analyses

All the data in the study are generated by three independent experiments with three replicates. Statistical analyses of the data were performed in Microsoft Office Excel 2019. Error bars in the graphs are standard errors of the mean (±SE). Experimental data were subjected to

Student's t-test analyses to determine the statistical significance between WT and *PRpnp* transgenic plants or between control and treatment sets.

Acknowledgments

SS thanks to junior and senior research fellowships and HC thanks faculty initiation grant (FIG-100677) by IITR.

Conflict of interest statement

The authors declare that they have no conflict of interest.

Author contributions

SS and HC conceived the project and designed the experiments. SS performed most of the experiments and analyzed the data; SG and HG performed subcellular localization; CK and SS analyzed the RNA-sequencing data; CK, LV, and JG conducted and analyzed the LC-MS/MS experiments; RDB and GTB performed thrips mortality bioassay; ZT assisted in recombinant protein purification for antibody generation; DKS gave substantial suggestions during experiments; SS wrote the manuscript; HC and AKS revised the manuscript. All authors read and approved the manuscript.

Data-availability

RNA-seq datasets related to this work have been deposited in Gene Expression Omnibus (GEO) with the accession number GSE208104.

Supplementary information

Figure S1: Confirmation of molecular cloning of expression cassette.

Figure S2: Procedure of development of transgenic *C. aurantifolia.*

Figure S3: Molecular characterization of putative *PRpnp* transgenic plants by duplex PCR and qRT-PCR.

Figure S4: Western blot analysis and assessment of PRpnp dual activity in transgenic *C. aurantifolia*

Figure S5: PCA and volcano plot of transcriptome profiles of WT and *PRpnp* transgenic *C. aurantifolia*.

Figure S6: Network analysis of enriched pathways in transgenic *C. aurantifolia*.

Figure S7: Heat map of DEGs in transgenic *C. aurantifolia*.

Table S1: Total recovered GUS positive transgenic *C. aurantifolia* plants.

Table S2: *De novo* transcriptome summary.

Table S3: List of up-regulated DEGs.

Table S4: List of down-regulated DEGs.

Table S5: List of primers.

Table S6: PCR conditions.

Table S7: Culture media composition.

References

1. Abbaraju, H.K., Gupta, R., Appenzeller, L.M., Fallis, L.P., Hazebroek, J., Zhu, G., Bourett, T.M., Howard, R.J., Weers, B., Lafitte, R.H. and Hakimi, S.M., 2022. A vegetative storage protein improves drought tolerance in maize. *Plant biotechnology journal*, *20*(2), p.374.
2. Abbott, W.S., 1925. A method of computing the effectiveness of an insecticide. *J. econ. Entomol*, *18*(2), pp.265-267.
3. Abe, H., Ohnishi, J., Narusaka, M., Seo, S., Narusaka, Y., Tsuda, S. and Kobayashi, M., 2008. Function of jasmonate in response and tolerance of Arabidopsis to thrip feeding. *Plant and cell physiology*, *49*(1), pp.68-80.
4. Abe, H., Shimoda, T., Ohnishi, J., Kugimiya, S., Narusaka, M., Seo, S., Narusaka, Y., Tsuda, S. and Kobayashi, M., 2009. Jasmonate-dependent plant defense restricts thrips performance and preference. *BMC plant biology*, *9*(1), pp.1-12.
5. Afitlhile, M.M., Fukushige, H., Nishimura, M. and Hildebrand, D.F., 2005. A defect in glyoxysomal fatty acid β-oxidation reduces jasmonic acid accumulation in Arabidopsis. *Plant Physiology and Biochemistry*, *43*(6), pp.603-609.
6. Altmann, M., Altmann, S., Rodriguez, P.A., Weller, B., Elorduy Vergara, L., Palme, J., Marín-de la Rosa, N., Sauer, M., Wenig, M., Villaécija-Aguilar, J.A. and Sales, J., 2020. Extensive signal integration by the phytohormone protein network. *Nature*, *583*(7815), pp.271-276.
7. Annadana, S., Peters, J., Gruden, K., Schipper, A., Outchkourov, N.S., Beekwilder, M.J., Udayakumar, M. and Jongsma, M.A., 2002. Effects of cysteine protease inhibitors on oviposition rate of the western flower thrips, Frankliniella occidentalis. *Journal of Insect Physiology*, *48*(7), pp.701-706.
8. Ashihara, H., Stasolla, C., Fujimura, T. and Crozier, A., 2018. Purine salvage in plants. *Phytochemistry*, *147*, pp.89-124.
9. Avice, J.C., Dily, F.L., Goulas, E., Noquet, C., Meuriot, F., Volenec, J.J., Cunningham, S.M., Sors, T.G., Dhont, C., Castonguay, Y. and Nadeau, P., 2003. Vegetative storage proteins in overwintering storage organs of forage legumes: roles and regulation. *Canadian Journal of Botany*, *81*(12), pp.1198-1212.
10. Bartlett, M.E. and Whipple, C.J., 2013. Protein change in plant evolution: tracing one thread connecting molecular and phenotypic diversity. *Frontiers in plant science*, *4*, p.382.

11. Bates, L.S., Waldren, R.P. and Teare, I.D., 1973. Rapid determination of free proline for water-stress studies. *Plant and soil*, *39*(1), pp.205-207.
12. Bhaskaran, S. and Savithramma, D.L., 2011. Co-expression of Pennisetum glaucum vacuolar Na+/H+ antiporter and Arabidopsis H+-pyrophosphatase enhances salt tolerance in transgenic tomato. *Journal of experimental botany*, *62*(15), pp.5561-5570.
13. Bhatnagar, N., Min, M.K., Choi, E.H., Kim, N., Moon, S.J., Yoon, I., Kwon, T., Jung, K.H. and Kim, B.G., 2017. The protein phosphatase 2C clade A protein OsPP2C51 positively regulates seed germination by directly inactivating OsbZIP10. *Plant Molecular Biology*, *93*(4), pp.389-401.
14. Bittner, F., Oreb, M. and Mendel, R.R., 2001. ABA3 is a molybdenum cofactor sulfurase required for activation of aldehyde oxidase and xanthine dehydrogenase in Arabidopsis thaliana. *Journal of Biological Chemistry*, *276*(44), pp.40381-40384.
15. Bradford, M.M., 1976. A rapid and sensitive method for the quantitation of microgram quantities of protein utilizing the principle of protein-dye binding. *Analytical biochemistry*, *72*(1-2), pp.248-254.
16. Castellano, BERNARDO., González, B., Finsen, B.R. and Zimmer, J.E.N.S., 1990. Histochemical demonstration of purine nucleoside phosphorylase (PNPase) in microglial and astroglial cells of adult rat brain. *Journal of Histochemistry & Cytochemistry*, *38*(11), pp.1535-1539.
17. Chaudhary, N.S., Shee, C., Islam, A., Ahmad, F., Yernool, D., Kumar, P. and Sharma, A.K., 2008. Purification and characterization of a trypsin inhibitor from Putranjiva roxburghii seeds. *Phytochemistry*, *69*(11), pp.2120-2126.
18. Chauvin, A., Caldelari, D., Wolfender, J.L. and Farmer, E.E., 2013. Four 13-lipoxygenases contribute to rapid jasmonate synthesis in wounded Arabidopsis thaliana leaves: a role for lipoxygenase 6 in responses to long-distance wound signals. *New Phytologist*, *197*(2), pp.566-575.
19. Chen, H., Chen, W., Zhou, J., He, H., Chen, L., Chen, H. and Deng, X.W., 2012. Basic leucine zipper transcription factor OsbZIP16 positively regulates drought resistance in rice. *Plant science*, *193*, pp.8-17.
20. Chen, L., Zhang, L., Xiang, S., Chen, Y., Zhang, H. and Yu, D., 2021. The transcription factor WRKY75 positively regulates jasmonate-mediated plant defense to necrotrophic fungal pathogens. *Journal of Experimental Botany*, *72*(4), pp.1473-1489.

21. Clemente, M., Corigliano, M.G., Pariani, S.A., Sánchez-López, E.F., Sander, V.A. and Ramos-Duarte, V.A., 2019. Plant serine protease inhibitors: biotechnology application in agriculture and molecular farming. *International journal of molecular sciences*, *20*(6), p.1345.
22. Cui, M., Zhang, W., Zhang, Q., Xu, Z., Zhu, Z., Duan, F. and Wu, R., 2011. Induced over-expression of the transcription factor OsDREB2A improves drought tolerance in rice. *Plant Physiology and Biochemistry*, *49*(12), pp.1384-1391.
23. de Ollas, C., Arbona, V. and Gómez-Cadenas, A., 2015. Jasmonic acid interacts with abscisic acid to regulate plant responses to water stress conditions. *Plant signaling & behavior*, *10*(12), p.e1078953.
24. Donkersley, P., Silva, F.W., Carvalho, C.M., Al-Sadi, A.M. and Elliot, S.L., 2018. Biological, environmental and socioeconomic threats to citrus lime production. *Journal of Plant Diseases and Protection*, *125*(4), pp.339-356.
25. Escobar-Bravo, R., Klinkhamer, P.G. and Leiss, K.A., 2017. Induction of jasmonic acid-associated defenses by thrips alters host suitability for conspecifics and correlates with increased trichome densities in tomato. *Plant and cell physiology*, *58*(3), pp.622-634.
26. Frebort, I., Kowalska, M., Hluska, T., Frébortová, J. and Galuszka, P., 2011. Evolution of cytokinin biosynthesis and degradation. *Journal of Experimental Botany*, *62*(8), pp.2431-2452.
27. Gao, F., Xiong, A., Peng, R., Jin, X., Xu, J., Zhu, B., Chen, J. and Yao, Q., 2010. OsNAC52, a rice NAC transcription factor, potentially responds to ABA and confers drought tolerance in transgenic plants. *Plant Cell, Tissue and Organ Culture (PCTOC)*, *100*(3), pp.255-262.
28. Giuliani, P., Zuccarini, M., Buccella, S., Peña-Altamira, L.E., Polazzi, E., Virgili, M., Monti, B., Poli, A., Rathbone, M.P., Iorio, P.D. and Ciccarelli, R., 2017. Evidence for purine nucleoside phosphorylase (PNP) release from rat C6 glioma cells. *Journal of Neurochemistry*, *141*(2), pp.208-221.
29. Gu, X.C., Chen, J.F., Xiao, Y., Di, P., Xuan, H.J., Zhou, X., Zhang, L. and Chen, W.S., 2012. Overexpression of allene oxide cyclase promoted tanshinone/phenolic acid production in Salvia miltiorrhiza. *Plant cell reports*, *31*(12), pp.2247-2259.
30. Haag, R. and Lewis, R.A., 1994. The partial purification and characterization of purine nucleoside phosphorylase from mammalian mitochondria. *Molecular and cellular biochemistry*, *135*(2), pp.129-136.

31. Haas, B.J., Papanicolaou, A., Yassour, M., Grabherr, M., Blood, P.D., Bowden, J., Couger, M.B., Eccles, D., Li, B., Lieber, M. and MacManes, M.D., 2013. De novo transcript sequence reconstruction from RNA-seq using the Trinity platform for reference generation and analysis. *Nature protocols*, *8*(8), pp.1494-1512.
32. Hamani, A.K.M., Wang, G., Soothar, M.K., Shen, X., Gao, Y., Qiu, R. and Mehmood, F., 2020. Responses of leaf gas exchange attributes, photosynthetic pigments and antioxidant enzymes in NaCl-stressed cotton (Gossypium hirsutum L.) seedlings to exogenous glycine betaine and salicylic acid. *BMC Plant Biology*, *20*(1), pp.1-14.
33. Hiscox, J.D. and Israelstam, G.F., 1979. A method for the extraction of chlorophyll from leaf tissue without maceration. *Canadian journal of botany*, *57*(12), pp.1332-1334.
34. Hodges, D.M., DeLong, J.M., Forney, C.F. and Prange, R.K., 1999. Improving the thiobarbituric acid-reactive-substances assay for estimating lipid peroxidation in plant tissues containing anthocyanin and other interfering compounds. *Planta*, *207*(4), pp.604-611.
35. Jefferson, R.A., Kavanagh, T.A. and Bevan, MW., 1987. GUS fusions: beta-glucuronidase as a sensitive and versatile gene fusion marker in higher plants. *The EMBO journal*, *6*(13), pp.3901-3907.
36. Jha, B., Mishra, A., Jha, A. and Joshi, M., 2013. Developing transgenic Jatropha using the SbNHX1 gene from an extreme halophyte for cultivation in saline wasteland. *PLoS One*, *8*(8), p.e71136.
37. Kang, J., Hwang, J.U., Lee, M., Kim, Y.Y., Assmann, S.M., Martinoia, E. and Lee, Y., 2010. PDR-type ABC transporter mediates cellular uptake of the phytohormone abscisic acid. *Proceedings of the National Academy of sciences*, *107*(5), pp.2355-2360.
38. Karimi, M., Inzé, D. and Depicker, A., 2002. GATEWAY™ vectors for Agrobacterium-mediated plant transformation. *Trends in plant science*, *7*(5), pp.193-195.
39. Katahira, R. and Ashihara, H., 2006. Role of adenosine salvage in wound-induced adenylate biosynthesis in potato tuber slices. *Plant physiology and biochemistry*, *44*(10), pp.551-555.

40. Kavi kishor, P.B. and Sreenivasulu, N.E.S.E., 2014. Is proline accumulation per se correlated with stress tolerance or is proline homeostasis a more critical issue?. *Plant, cell & environment*, *37*(2), pp.300-311.
41. Kim, H., Seomun, S., Yoon, Y. and Jang, G., 2021. Jasmonic acid in plant abiotic stress tolerance and interaction with abscisic acid. *Agronomy*, *11*(9), p.1886.
42. Kim, S., Choi, H.I., Ryu, H.J., Park, J.H., Kim, M.D. and Kim, S.Y., 2004. ARIA, an Arabidopsis arm repeat protein interacting with a transcriptional regulator of abscisic acid-responsive gene expression, is a novel abscisic acid signaling component. *Plant physiology*, *136*(3), pp.3639-3648.
43. Kondo, M., Yamaoka, T., Honda, S., Miwa, Y., Katashima, R., Moritani, M., Yoshimoto, K., Hayashi, Y. and Itakura, M., 2000. The rate of cell growth is regulated by purine biosynthesis via ATP production and G1 to S phase transition. *The Journal of Biochemistry*, *128*(1), pp.57-64.
44. Koo, A.J., Chung, H.S., Kobayashi, Y. and Howe, G.A., 2006. Identification of a Peroxisomal Acyl-activating Enzyme Involved in the Biosynthesis of Jasmonic Acid in Arabidopsis. *Journal of Biological Chemistry*, *281*(44), pp.33511-33520.
45. Kuipers, A.G. and Jongsma, M.A., 2004. Isolation and molecular characterization of cathepsin L-like cysteine protease cDNAs from western flower thrips (Frankliniella occidentalis). *Comparative Biochemistry and Physiology Part B: Biochemistry and Molecular Biology*, *139*(1), pp.65-75.
46. Li, B. and Dewey, C.N., 2011. RSEM: accurate transcript quantification from RNA-Seq data with or without a reference genome. *BMC bioinformatics*, *12*(1), pp.1-16.
47. Li, J., Chen, L., Ding, X., Fan, W. and Liu, J., 2022. Transcriptome Analysis Reveals Crosstalk between the Abscisic Acid and Jasmonic Acid Signaling Pathways in Rice-Mediated Defense against Nilaparvata lugens. *International Journal of Molecular Sciences*, *23*(11), p.6319.
48. Liu, Y., Ahn, J.E., Datta, S., Salzman, R.A., Moon, J., Huyghues-Despointes, B., Pittendrigh, B., Murdock, L.L., Koiwa, H. and Zhu-Salzman, K., 2005. Arabidopsis vegetative storage protein is an anti-insect acid phosphatase. *Plant Physiology*, *139*(3), pp.1545-1556.
49. Liu, Y., Heying, E. and Tanumihardjo, S.A., 2012. History, global distribution, and nutritional importance of citrus fruits. *Comprehensive reviews in Food Science and Food safety*, *11*(6), pp.530-545.

50. Livak, K.J. and Schmittgen, T.D., 2001. Analysis of relative gene expression data using real-time quantitative PCR and the 2− ΔΔCT method. *methods*, *25*(4), pp.402-408.

51. Love, M.I., Huber, W. and Anders, S., 2014. Moderated estimation of fold change and dispersion for RNA-seq data with DESeq2. *Genome biology*, *15*(12), pp.1-21.

52. Ma, X.J., Fu, J.D., Tang, Y.M., Yu, T.F., Yin, Z.G., Chen, J., Zhou, Y.B., Chen, M., Xu, Z.S. and Ma, Y.Z., 2020. GmNFYA13 improves salt and drought tolerance in transgenic soybean plants. *Frontiers in Plant Science*, p.1584.

53. Maere, S., Heymans, K. and Kuiper, M., 2005. BiNGO: a Cytoscape plugin to assess overrepresentation of gene ontology categories in biological networks. *Bioinformatics*, *21*(16), pp.3448-3449.

54. Medeiros, A.H., Franco, F.P., Matos, J.L., de Castro, P.A., Santos-Silva, L.K., Henrique-Silva, F., Goldman, G.H., Moura, D.S. and Silva-Filho, M.C., 2012. Sugarwin: a sugarcane insect-induced gene with antipathogenic activity. *Molecular plant-microbe interactions*, *25*(5), pp.613-624.

55. Morgan, J.A., 1984. Interaction of water supply and N in wheat. *Plant physiology*, *76*(1), pp.112-117.

56. Moura, D.S. and Ryan, C.A., 2001. Wound-inducible proteinase inhibitors in pepper. Differential regulation upon wounding, systemin, and methyl jasmonate. *Plant Physiology*, *126*(1), pp.289-298.

57. Neuwirth, E. and Neuwirth, M.E., 2014. Package 'RColorBrewer'. *ColorBrewer Palettes*.

58. Omar, A.A., Song, W.Y. and Grosser, J.W., 2007. Introduction of Xa21, a Xanthomonas-resistance gene from rice, into 'Hamlin'sweet orange [Citrus sinensis (L.) Osbeck] using protoplast-GFP co-transformation or single plasmid transformation. *The Journal of Horticultural Science and Biotechnology*, *82*(6), pp.914-923.

59. Patel, R.K. and Jain, M., 2012. NGS QC Toolkit: a toolkit for quality control of next generation sequencing data. *PloS one*, *7*(2), p.e30619.

60. Pedley, A.M. and Benkovic, S.J., 2017. A new view into the regulation of purine metabolism: the purinosome. *Trends in biochemical sciences*, *42*(2), pp.141-154.

61. Pigolev, A.V., Miroshnichenko, D.N., Pushin, A.S., Terentyev, V.V., Boutanayev, A.M., Dolgov, S.V. and Savchenko, T.V., 2018. Overexpression of Arabidopsis

OPR3 in hexaploid wheat (Triticum aestivum L.) alters plant development and freezing tolerance. *International journal of molecular sciences*, *19*(12), p.3989.

62. Quéméneur, L., Gerland, L.M., Flacher, M., Ffrench, M., Revillard, J.P. and Genestier, L., 2003. Differential control of cell cycle, proliferation, and survival of primary T lymphocytes by purine and pyrimidine nucleotides. *The Journal of Immunology*, *170*(10), pp.4986-4995.
63. Rubio, R. and Berne, R.M., 1980. Localization of purine and pyrimidine nucleoside phosphorylases in heart, kidney, and liver. *American Journal of Physiology-Heart and Circulatory Physiology*, *239*(6), pp.H721-H730.
64. Schoor, S., Farrow, S., Blaschke, H., Lee, S., Perry, G., von Schwartzenberg, K., Emery, N. and Moffatt, B., 2011. Adenosine kinase contributes to cytokinin interconversion in Arabidopsis. *Plant Physiology*, *157*(2), pp.659-672.
65. Senthilkumar, R., Cheng, C.P. and Yeh, K.W., 2010. Genetically pyramiding protease-inhibitor genes for dual broad-spectrum resistance against insect and phytopathogens in transgenic tobacco. *Plant biotechnology journal*, *8*(1), pp.65-75.
66. Seo, M., Peeters, A.J., Koiwai, H., Oritani, T., Marion-Poll, A., Zeevaart, J.A., Koornneef, M., Kamiya, Y. and Koshiba, T., 2000. The Arabidopsis aldehyde oxidase 3 (AAO3) gene product catalyzes the final step in abscisic acid biosynthesis in leaves. *Proceedings of the National Academy of Sciences*, *97*(23), pp.12908-12913.
67. Sidhu, G.P.S., Singh, H.P., Batish, D.R. and Kohli, R.K., 2017. Alterations in photosynthetic pigments, protein, and carbohydrate metabolism in a wild plant Coronopus didymus L.(Brassicaceae) under lead stress. *Acta Physiologiae Plantarum*, *39*(8), pp.1-9.
68. Song, Z., Yang, Q., Dong, B., Li, N., Wang, M., Du, T., Liu, N., Niu, L., Jin, H., Meng, D. and Fu, Y., 2022. Melatonin enhances stress tolerance in pigeon pea by promoting flavonoid enrichment, particularly luteolin in response to salt stress. *Journal of Experimental Botany*.
69. Srinivasan, T. and Kirti, P.B., 2012. Protease inhibitors and stress tolerance. *Funct Plant Sci Biotechnol*, *6*(1), pp.59-66.
70. Srinivasan, T., Kumar, K.R.R. and Kirti, P.B., 2009. Constitutive expression of a trypsin protease inhibitor confers multiple stress tolerance in transgenic tobacco. *Plant and Cell Physiology*, *50*(3), pp.541-553.
71. Tegeder, M. and Masclaux-Daubresse, C., 2018. Source and sink mechanisms of nitrogen transport and use. *New phytologist*, *217*(1), pp.35-53.

72. Verma, P., Patel, G.K., Kar, B. and Sharma, A.K., 2017. A case of neofunctionalization of a Putranjiva roxburghii PNP protein to trypsin inhibitor by disruption of PNP-UDP domain through an insert containing inhibitory site. *Plant Science*, *260*, pp.19-30.
73. Verma, P., Varshney, R., Yadav, S.P.S., Kar, B., Roy, P. and Sharma, A.K., 2022. SAXS Analysis and Characterization of Anticancer Activity of PNP-UDP Family Protein from Putranjiva roxburghii. *The Protein Journal*, pp.1-13.
74. Vishwakarma, K., Upadhyay, N., Kumar, N., Yadav, G., Singh, J., Mishra, R.K., Kumar, V., Verma, R., Upadhyay, R.G., Pandey, M. and Sharma, S., 2017. Abscisic acid signaling and abiotic stress tolerance in plants: a review on current knowledge and future prospects. *Frontiers in plant science*, *8*, p.161.
75. Wang, J., Li, Q., Mao, X., Li, A. and Jing, R., 2016. Wheat transcription factor TaAREB3 participates in drought and freezing tolerances in Arabidopsis. *International journal of biological sciences*, *12*(2), p.257.
76. Warnes, G.R., Bolker, B., Bonebakker, L., Gentleman, R., Huber, W., Liaw, A., Lumley, T., Maechler, M., Magnusson, A., Moeller, S. Schwartz, M., and Venables, B., 2022. gplots: Various R Programming Tools for Plotting Data. R package version 3.1.3.
77. Xu, Z., Zhou, G. and Shimizu, H., 2010. Plant responses to drought and rewatering. *Plant signaling & behavior*, *5*(6), pp.649-654.
78. Yang, W., Devaiah, S.P., Pan, X., Isaac, G., Welti, R. and Wang, X., 2007. AtPLAI is an acyl hydrolase involved in basal jasmonic acid production and Arabidopsis resistance to Botrytis cinerea. *Journal of Biological Chemistry*, *282*(25), pp.18116-18128.
79. Yao, P.L., Hwang, M.J., Chen, Y.M. and Yeh, K.W., 2001. Site-directed mutagenesis evidence for a negatively charged trypsin inhibitory loop in sweet potato sporamin. *FEBS letters*, *496*(2-3), pp.134-138.
80. Yu, C.S., Chen, Y.C., Lu, C.H. and Hwang, J.K., 2006. Prediction of protein subcellular localization. *Proteins: Structure, Function, and Bioinformatics*, *64*(3), pp.643-651.
81. Zhang, L., Zhang, L., Xia, C., Zhao, G., Liu, J., Jia, J. and Kong, X., 2015. A novel wheat bZIP transcription factor, TabZIP60, confers multiple abiotic stress tolerances in transgenic Arabidopsis. *Physiologia plantarum*, *153*(4), pp.538-554.

82. Zhang, X., Chen, Y., Lin, X., Hong, X., Zhu, Y., Li, W., He, W., An, F. and Guo, H., 2013. Adenine phosphoribosyl transferase 1 is a key enzyme catalyzing cytokinin conversion from nucleobases to nucleotides in Arabidopsis. *Molecular plant*, *6*(5), pp.1661-1672.
83. Zhao, H., Chiaro, C.R., Zhang, L., Smith, P.B., Chan, C.Y., Pedley, A.M., Pugh, R.J., French, J.B., Patterson, A.D. and Benkovic, S.J., 2015a. Quantitative Analysis of Purine Nucleotides Indicates That Purinosomes Increase de Novo Purine Biosynthesis. *Journal of Biological Chemistry*, *290*(11), pp.6705-6713.
84. Zhao, H., Ullah, H., McNeill, M.R., Du, G., Hao, K., Tu, X. and Zhang, Z., 2019. Inhibitory effects of plant trypsin inhibitors Msti-94 and Msti-16 on Therioaphis trifolii (Monell)(Homoptera: Aphididae) in Alfalfa. *Insects*, *10*(6), p.154.
85. Zhao, Q., Fan, Z., Qiu, L., Che, Q., Wang, T., Li, Y. and Wang, Y., 2020. MdbHLH130, an apple bHLH transcription factor, confers water stress resistance by regulating stomatal closure and ROS homeostasis in transgenic tobacco. *Frontiers in plant science*, *11*, p.543696.
86. Zhao, Y., Chan, Z., Gao, J., Xing, L., Cao, M., Yu, C., Hu, Y., You, J., Shi, H., Zhu, Y. and Gong, Y., 2015b. ABA receptor PYL9 promotes drought resistance and leaf senescence. *Proceedings of the National Academy of Sciences*, *113*(7), pp.1949-1954.
87. Zhou, W., Yao, Y., Scott, A.J., Wilder-Romans, K., Dresser, J.J., Werner, C.K., Sun, H., Pratt, D., Sajjakulnukit, P., Zhao, S.G. and Davis, M., 2020. Purine metabolism regulates DNA repair and therapy resistance in glioblastoma. *Nature communications*, *11*(1), pp.1-14.
88. Zubair, M., Latif, A., Rao, A.Q., Azam, S., Shahid, N., Samiullah, T.R., Yasmeen, A., Shahid, A.A., Nasir, I.A. and Husnain, T., 2019. A combinational approach of enhanced methanol production and double Bt genes for broad spectrum insect resistance in transgenic cotton. *Molecular biotechnology*, *61*(9), pp.663-673.

Figure legends:

Figure 1 Modular structure and subcellular localization of PRpnp. (a) PRpnp belongs to PNP family and consists of 288 amino acids. The PNP-UDP family domain in PRpnp is disrupted by a 46 amino acid insert. The attainment of trypsin inhibitory property through insert does not disturb the tertiary structure of PRpnp, suggesting its neofunctionalization due to the evolutionary needs of plant defense. TIL-Trypsin inhibitory loop. (b) PRpnp was localized in the nucleus and cytosol. *Agrobacterium* strain GV3101 harboring pB7FWG2-35S::PRpnp-GFP plasmid was infiltrated in *N. benthamiana* pavement cells. Live cell images were captured with laser-scanning confocal microscopy. (I) Transient expression of PRpnp-GFP protein, (II) RFP fluorescent signal, (III) Staining of the nuclei by DAPI, and (IV) Merged image of PRpnp-GFP, RFP, and DAPI channel. The GFP, RFP, and DAPI channels were excited at 488 nm, 552 nm, and 405 nm. The scale bar represents 36.2 μm.

Figure 2 Leaf disc senescence assays showed enhanced multiple stress tolerance in *PRpnp* transgenic *C. aurantifolia.* (a) Leaf discs were floated in media supplemented with 200 mM NaCl and 300 mM NaCl for 48 h and 72 h. (b) Leaf discs were evaluated against oxidative stress by adding 50 mM H_2O_2 to the media for 48 h. (c) Response of leaf discs was also tested against alkaline pH. To mimic higher alkalinity, the pH of the media was set to 9. For control, the leaf discs were incubated in ½ strength Hoagland solution; pH=5.8. In all the tested conditions, WT leaf discs showed a distinctly high level of bleaching, thus, indicating their low stress tolerance compared to transgenic. (d, e, f) Chlorophylls (a and b) and carotenoid content of WT and transgenic leaf discs were estimated and compared under control and stressed conditions; (d) salt stress, (e) oxidative stress, and (f) alkaline stress. All the transgenic leaf discs showed more chlorophylls and carotenoid content under stressed conditions over WT. Data represent means ± SE (n=3) of three biologically independent experiments. Significant differences between WT and transgenic lines were calculated using Student's *t*-test, **P*-value < 0.05 and ***P*-value < 0.01.

Figure 3 *PRpnp* overexpression enhances salt tolerance also under soil conditions. (a) Photographs of growth of WT and transgenic plant under salt stress at indicated time points. 0 day (0 d) represents plant conditions before stress treatment. Severe salt stress-induced symptoms in WT ultimately led to plant death; however, transgenic plants survived with no or little effect. Red arrows indicate salt stress-induced damage. (b) proline and (c)

malondialdehyde (MDA) content in WT and A17, A19, and A21 transgenic plants at regular intervals. Transgenic plants showed significantly higher levels of proline and lower levels of MDA relative to WT. Data represent means ± SE (n=3) of three biologically independent experiments. Significant differences between WT and transgenic lines were calculated using Student's *t*-test, **P*-value < 0.05 and ***P*-value < 0.01.

Figure 4 *PRpnp* overexpression enhances drought tolerance. (a) Phenotype of WT and transgenic plants under drought stress at the indicated time points. WT showed early and deleterious drought-induced symptoms along with delayed recovery upon reirrigation. However, transgenic plants survived all the phases of the experiment and showed quick recovery. Red arrows indicate new leaf development during drought stress. Zoomed view (ZV) shows delayed recovery in WT and new foliage development in transgenic plants upon rewatering. (b) proline content, (c) lipid peroxidation rates (MDA), and (d) relative water contents (RWC) of WT and A22, A24, and A25 transgenic plants at regular intervals. Transgenic plants showed relatively higher proline levels and RWC and a lower increase in MDA levels. Data represent means ± SE (n=3) of three biologically independent experiments. Significant differences between WT and transgenic lines were calculated using Student's *t*-test, **P*-value < 0.05 and ***P*-value < 0.01.

Figure 5 *PRpnp* overexpression enhances resistance against *P. demoleus* larvae. WT and transgenic leaves (plant A2, A6, and A11) were fed to five-second instar larvae. Infestation of the larvae at (a) 4 day-post-hatching (DPH), (b) 9 DPH, and (c) 12 DPH. Transgenic-fed larvae showed significantly visible retarded growth with delayed instar development between 9 and 12 DPH. (d) A comparison of body weights at the indicated time and (e) mortality (%) at 12 DPH of WT- and transgenic-fed larvae. Lower body weights and increased mortality of transgenic-fed larvae signify enhanced resistance in transgenic plants. Data represent means ± SE (n=3) of three biologically independent experiments. The asterisks represent a significant difference between WT and transgenic lines were calculated using Student's *t*-test, **P*-value < 0.05 and ***P*-value < 0.01.

†For representation, a comparative larval infestation on WT and transgenic leaves A2 is shown.

Figure 6 *PRpnp* overexpression enhances resistance against adult *S. citri*. Adult thrips collected from the infected plant were fed to prepared WT and transgenic leaves and

corrected mortality; CM (%) was monitored for 72h. (a) Experimental setup for bioassay. (b) Microscopic image of *S. citri* infestation on the detached leaf. Inset- zoomed image of an adult thrips. Photographs of (c) healthy and (d) dead thrips fed on WT and transgenic (TR) leaves, respectively. (e) Increased CM (%) of adult *S. citri* in A2, A6, and A11 represents enhanced resistance in *PRpnp* transgenic plants. Data represent means ± SE (n=3) of three biologically independent experiments.

Figure 7 Phytohormones quantification by LC-MS/MS in WT and *PRpnp* transgenic plants. (a) abscisic acid (ABA), (b) jasmonic acid (JA), and (c) cytokinin (CK; tZ). *PRpnp* overexpression caused more endogenous accumulation of tested phytohormones under normal growth conditions. Measurements are averaged over three replicates. Error bars represent ± SE.

Supplementary figure legends:

Figure S1 Confirmation of molecular cloning of expression cassette in pBSSK(+) cloning vector and pCAMBIA2301 binary vector and vector construct of pCAMBIA2301-2x35S::PRpnp. (a) pBSSK(+)-2x35S::PRpnp construct was digested with respective restriction enzymes to release the cloned fragments. M- marker (SD010; GeneDireX, Inc.); L1- CaMV 35S promoter (enhanced) (774 bps); L2- *PRpnp* gene (867 bps); L3- T-nos (253 bps). (b) pCAMBIA2301-2x35S::PRpnp construct was digested with *KpnI* and *XbaI* and the complete expression cassette of 1894 bps was released, showing successful molecular cloning in binary vector; M- marker (SD010; GeneDireX, Inc.); L1- digested empty pCAMBIA2301; L2- *PRpnp* expression cassette. (c) Schematic depiction of pCAMBIA2301 binary vector construct used to overexpress *PRpnp*. One of the most effective regulatory sequences i.e., CaMV 35S promoter (enhanced), cloned in *KpnI-HindII* sites, was used to drive the constitutive expression of *PRpnp* in *C. aurantifolia. PRpnp* gene was cloned in *HindIII-BamHI* sites and transcriptional terminator, T-nos was cloned as *BamHI-XbaI* fragment. LB- left border; P2xCaMV 35S- CaMV 35S promoter (enhanced); *nptII*- neomycin phosphotransferase gene; CaMV P(A)- CaMV poly(A) signal; *PRpnp* - *Putranjiva roxburghii* purine nucleoside phosphorylase gene; T-nos- nopaline synthase terminator; PCaMV 35S- CaMV 35S promoter; *gusA*- β-glucuronidase gene; RB- right border.

Figure S2 Procedure of development of transgenic *C. aurantifolia* Cv. Pramalini overexpressing *PRpnp* by *Agrobacterium*- mediated transformation. (a) 4- week-old pre-treated epicotyls were infected with *Agrobacterium* strain EHA105 harboring pCAMBIA2301-2x35S::PRpnp overexpression construct and cultured on SMA2NB media for 2 days. Inset- zoomed view of epicotyl showing the oblique cut pattern at the end. (b) Epicotyl was regenerated after ~2 weeks of incubation on MRNB1 media. (c) Epicotyl showed a highly efficient regeneration on MRNB1 media after ~5 weeks of incubation. (d, e) GUS histochemical assay of the basal portion of regenerated shoots; (d) No GUS activity and (e) blue color indicating positive GUS activity in shoots regenerated from untransformed and transformed epicotyl, respectively. (f, g) Stages of *in-vitro* micrografting of the transgenic shoot; (f) scion and rootstock (3-weeks-old *C. jambhiri)* was prepared and (g) successful graft union between scion-rootstock was developed after 2 weeks of incubation in ML media. (h) Roots were developed in transgenic shoots after 3-4 weeks on MR media. (i) The whole transgenic plant was transferred to the greenhouse for hardening.

Figure S3 Molecular characterization of putative *PRpnp* transgenic plants by duplex PCR and qRT-PCR. (a) The genomic DNA was isolated from WT and putative transgenic plants and *PRpnp* and *nptII* genes were amplified by duplex PCR. M-marker (SD010; GeneDireX, Inc.); WT- wild-type; L1-L14- transgenic plants; L15- NTC; L16- positive control (pCAMBIA2301-2x35S::PRpnp). For representation, the duplex PCR amplification of *PRpnp* and *nptII* genes in 14 arbitrarily selected transgenic plants is shown. (b) Ct values of *PRpnp* were compared in WT and transgenic plants. qRT-PCR of housekeeping gene i.e., cytochrome oxidase (*cox*) showed similar expression patterns across all the plants while *PRpnp* expression was not detected in WT and varied in different transgenic plants. WT- wild-type and TR- transgenic plants. qRT-PCR was conducted using two replicates and the error bar represents the mean ± SE. The fold change in gene expression was calculated relative to WT plants, whose Ct value for *PRpnp* was set to 40 (data not shown). Because *PRpnp* gene is ectopic to *C. aurantifolia,* it was undetected (UD) in WT plants by qRT-PCR; however, its expression was detected in transgenic plants and thus, confirms the transgene expression.

Figure S4 Characterization of transgenic *C. aurantifolia* by Western blot analysis and assessment of PRpnp dual activity. (a) Total leaf protein (10 µg) from WT and *PRpnp* transgenic plants was first probed with anti-PRpnp antibody and then with anti-rabbit IgG,

HRP linked antibody. No band was detected in WT; however, the expression of PRpnp protein was confirmed by the appearance of a clear ~34 kDa band in transgenic plants. WT- wild-type and TR- transgenic plants. Blot 1- M- Marker (PM007; GeneDireX, Inc.), WT, A2, A6, and A11; Blot 2- A17, A19, A21, A22, A24, A25, A28, A30, and A32. (b) Total protein extract (200 µg) from WT and transgenic plants A2, A6, and A11 were isolated. (I) The PNP activity was assayed by an increase in OD at 293 nm and (II) Quantitative analysis of trypsin inhibitory activity as inhibition percentage (I%). The OD of the reaction mixture was recorded at 410 nm. Transgenic protein fractions showed PNP and trypsin inhibitory activities. Data represent means ± SE (n=3) of three biologically independent experiments.

Figure S5 (a) PCA and (b) volcano plot of transcriptome profiles of WT and *PRpnp* transgenic *C. aurantifolia* with two replicates under normal growth conditions.

Figure S6 Network analysis showing the enriched pathways of the up-regulated (a-e) and down-regulated (f-h) DEGs. (a) Response to stimulus, (b) cellular process, (c) cellular metabolic process, (d) developmental process, and (e) transport; (f) developmental process, (g) cell wall organization, and (h) metabolic process in *PRpnp* transgenic *C. aurantifolia.*

Figure S7 Heat map showing the hierarchical clustering of the up-regulated (a-i) and down-regulated (j-m) DEGs. (a) Phytohormone biosynthesis and signaling, (b) plant defense and immunity, (c) transcription factors, (d) transporters, (e) cell cycle, (f) DNA repair, (g) photosynthesis, (h) development, and (i) metabolism; (j) hormone signaling, (k) lipid metabolism, (l) cell fate, and (m) catabolism in *PRpnp* transgenic *C. aurantifolia* (TR). The green color represents downregulation and the red color represents relatively high expression. TMM normalized FPKM values were used to construct the heat maps. See color legend for expression levels.

Tables:

Table 1 Differentially regulated genes in *PRpnp* transgenic *C. aurantifolia* related to ABA biosynthesis and signaling.

Gene	Description	F.C	Reference
AAO3	Abscisic-aldehyde oxidase	2.98	Seo et al., 2000
ABA3	Molybdenum cofactor sulfurase	5.17	Bittner et al., 2001
ARIA	Arm repeat protein interacting with ABF2	10.52	Kim et al., 2004
NAC052	NAC domain containing protein 52	8.50	Gao et al., 2010
ABCG40	ABC transporter G family member 40	3.14	Kang et al., 2010
BZIP16	bZIP transcription factor 16	3.33	Chen et al., 2012
BZIP60	bZIP transcription factor 60	6.36	Zhang et al., 2015
PYL9	Abscisic acid receptor PYL9	5.41	Zhao et al., 2015b
AREB3	Abscisic acid-insensitive 5-like protein 2	10.21	Wang et al., 2016
PP2C51	Protein phosphatase 2C 51	-6.60	Bhatnagar et al., 2017
BHLH130	Transcription factor bHLH130	3.78	Zhao et al., 2020

Table 2 Differentially regulated genes in *PRpnp* transgenic *C. aurantifolia* related to JA biosynthesis and signaling.

Gene	Description	F.C	Reference
KAT2	3-ketoacyl-CoA thiolase 2	5.33	Afitlhile et al., 2005
4CLL5 (*OPCL1*)	OPC-8:0-CoA ligase 1	11.50	Koo et al., 2006
4CLL7	4-coumarate--CoA ligase-like 7	7.81	
4CLL9	4-coumarate--CoA ligase-like 9	3.66	
PLA1	Phospholipase A I	9.93	Yang et al., 2007
AOC3	Allene oxide cyclase 3	4.43	Gu et al., 2012
LOX6	Lipoxygenase 6	5.61	Chauvin et al., 2013
OPR3	12-oxophytodienoate reductase 3	7.17	Pigolev et al., 2018
WRKY75	Probable WRKY transcription factor 75	2.69	Chen et al., 2021

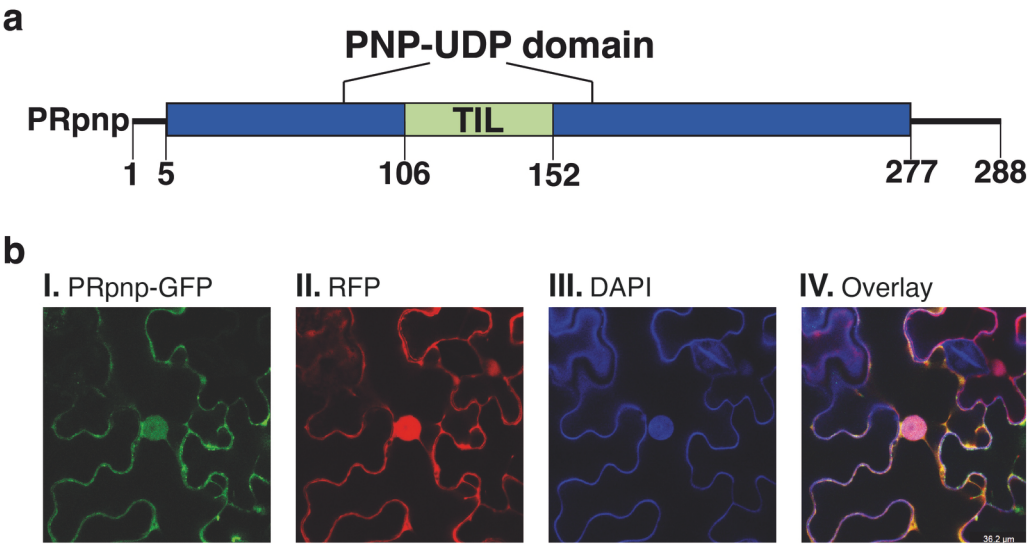

Manuscript image 1.jpg

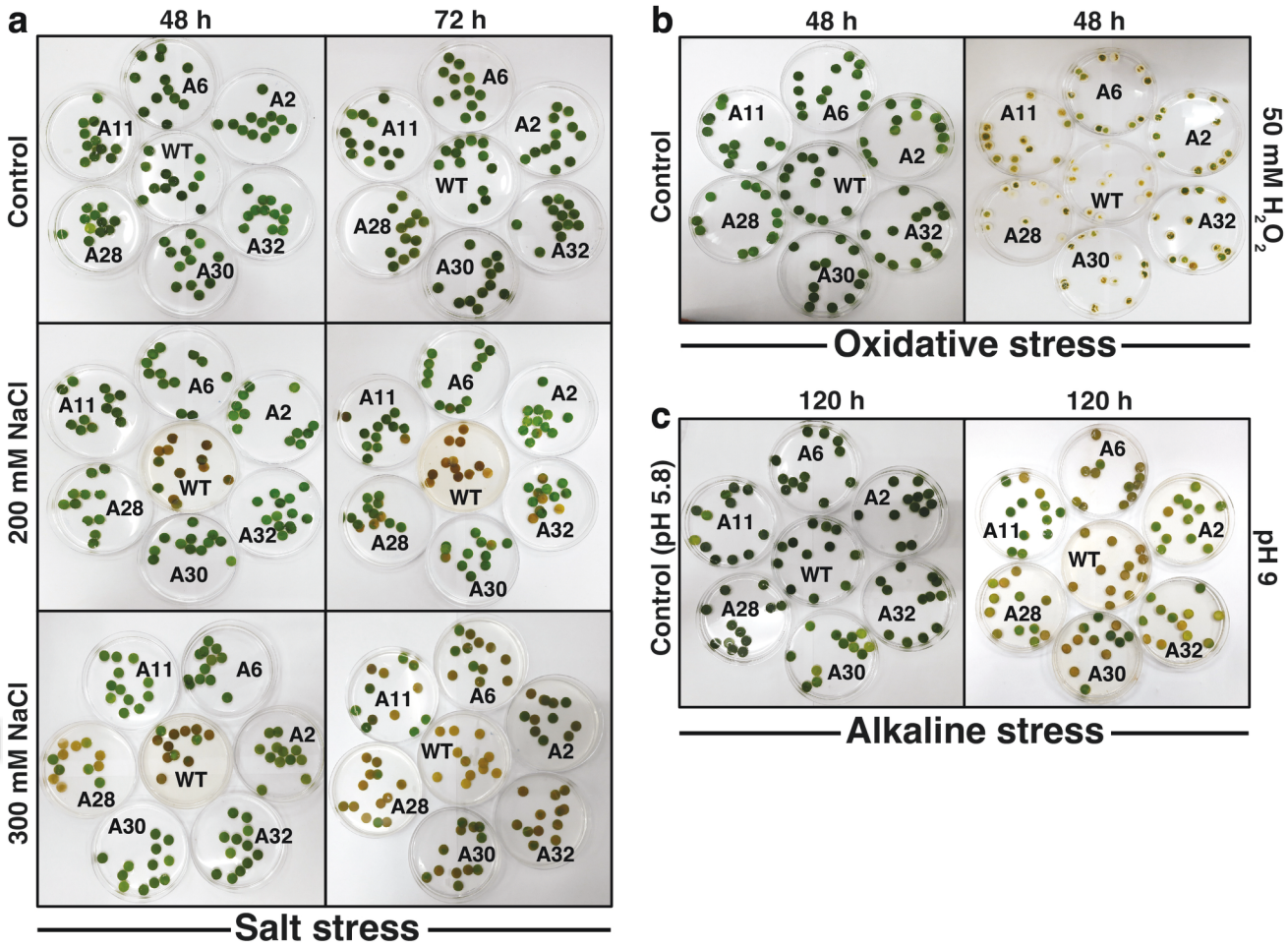

Manuscript image 2.jpg

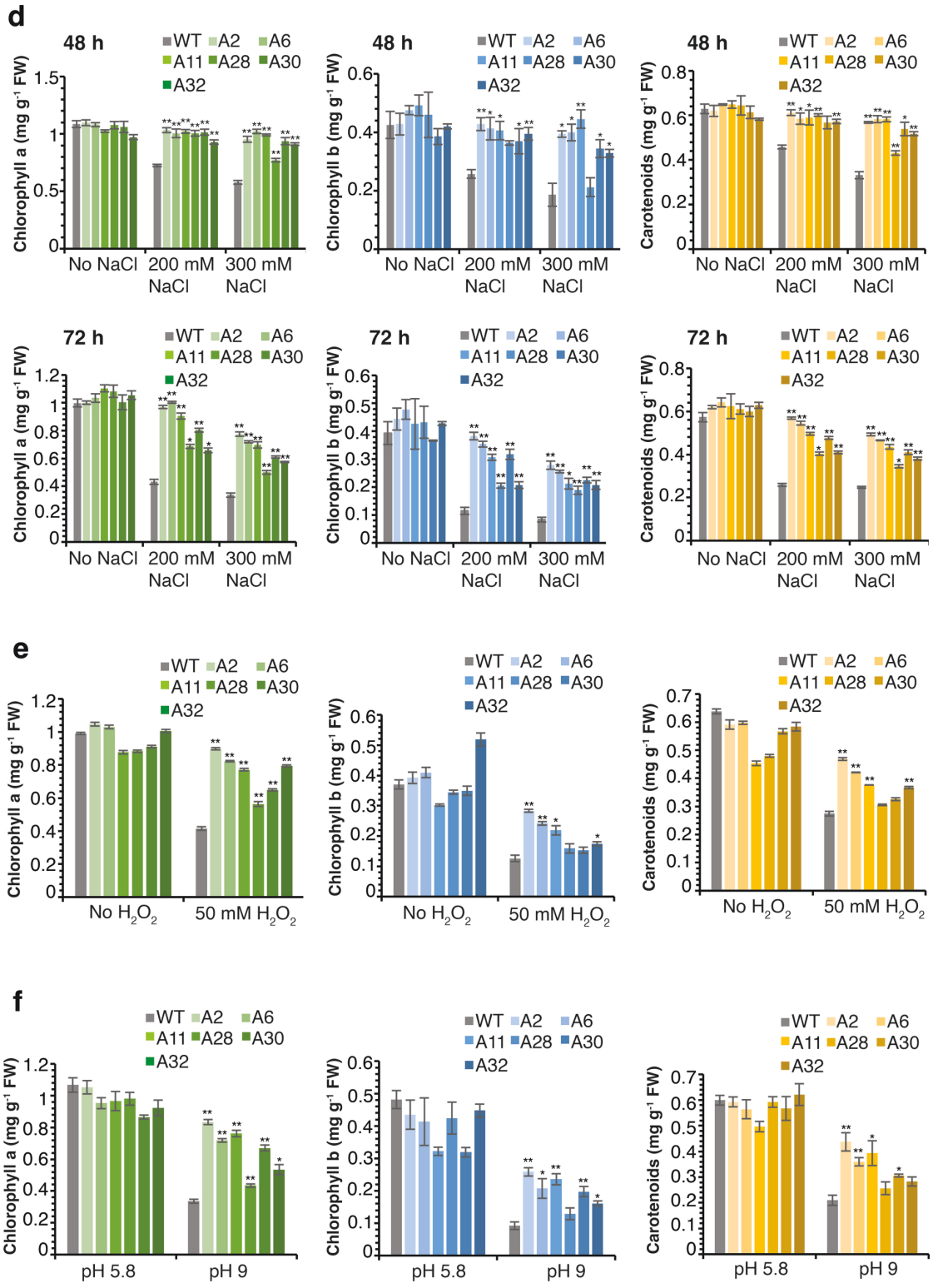

Manuscript image 2_Continued.jpg

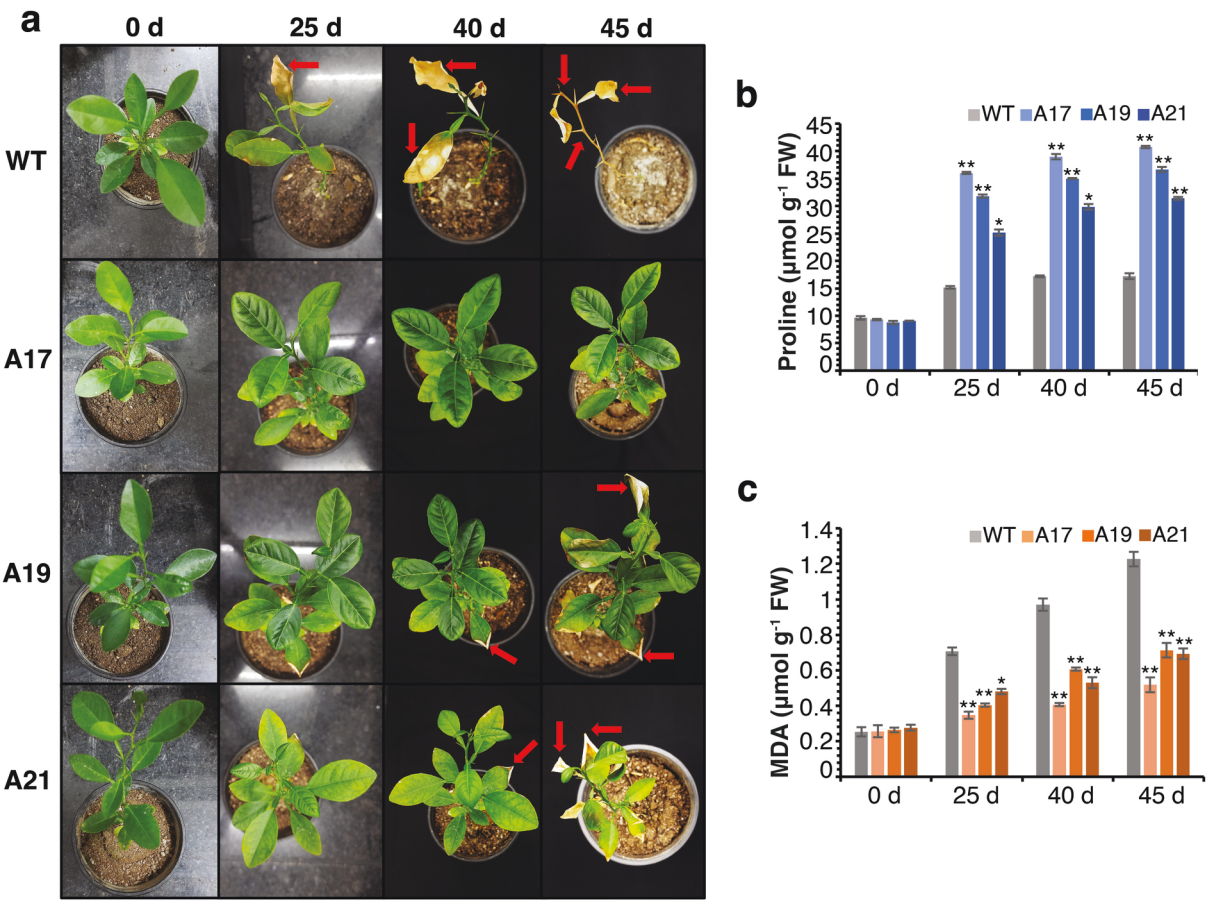

Manuscript image 3.jpg

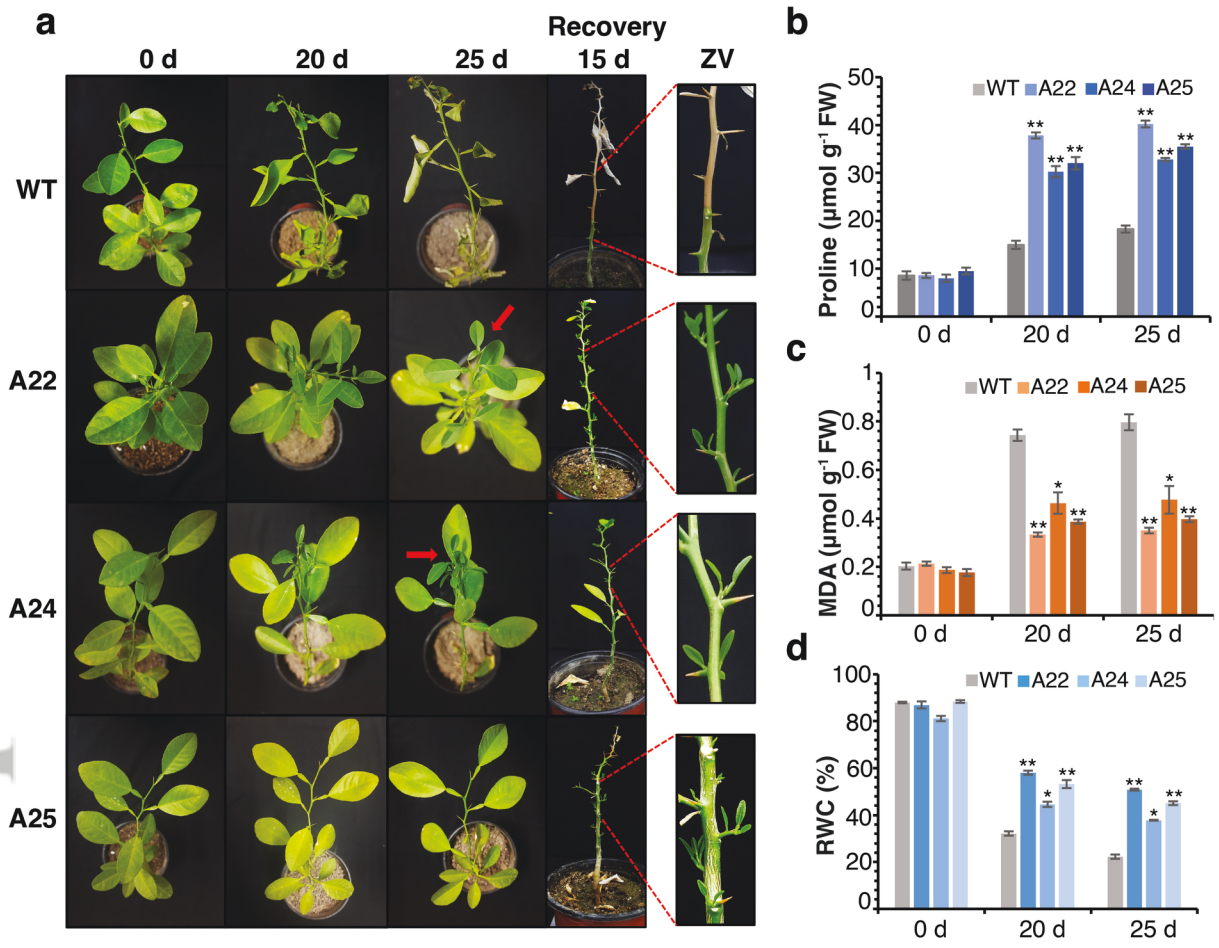

Manuscript image 4.jpg

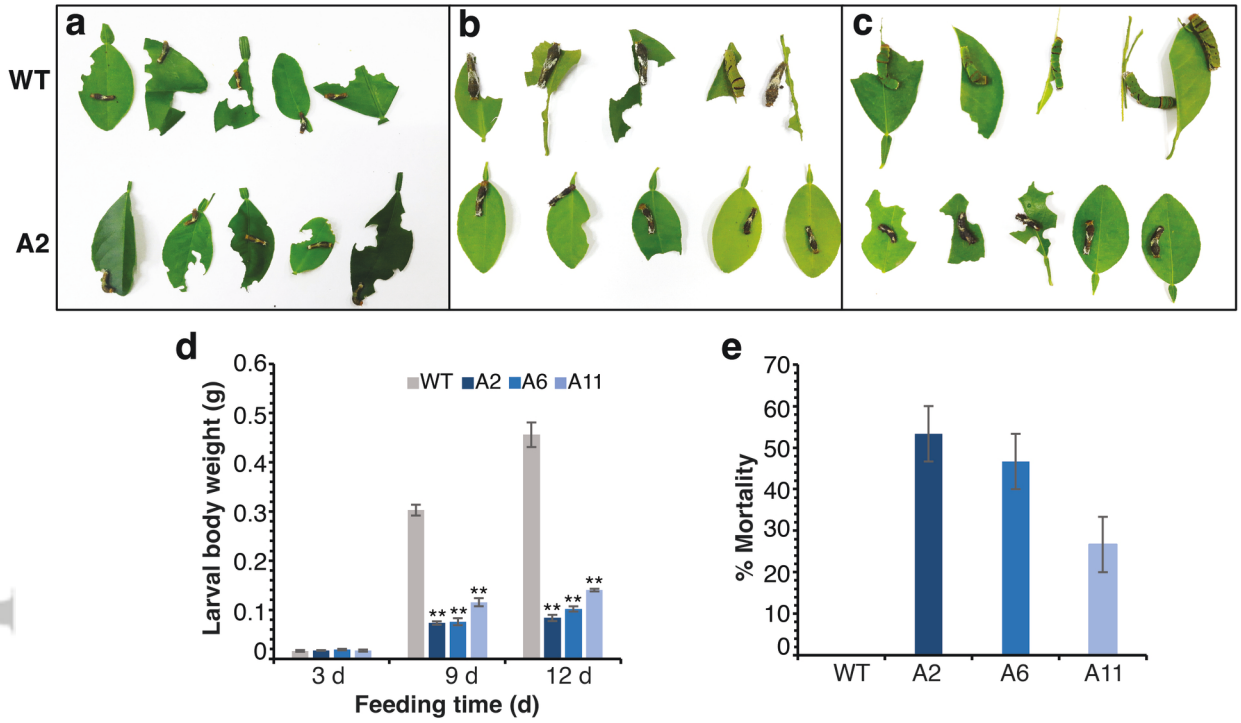

Manuscript image 5.jpg

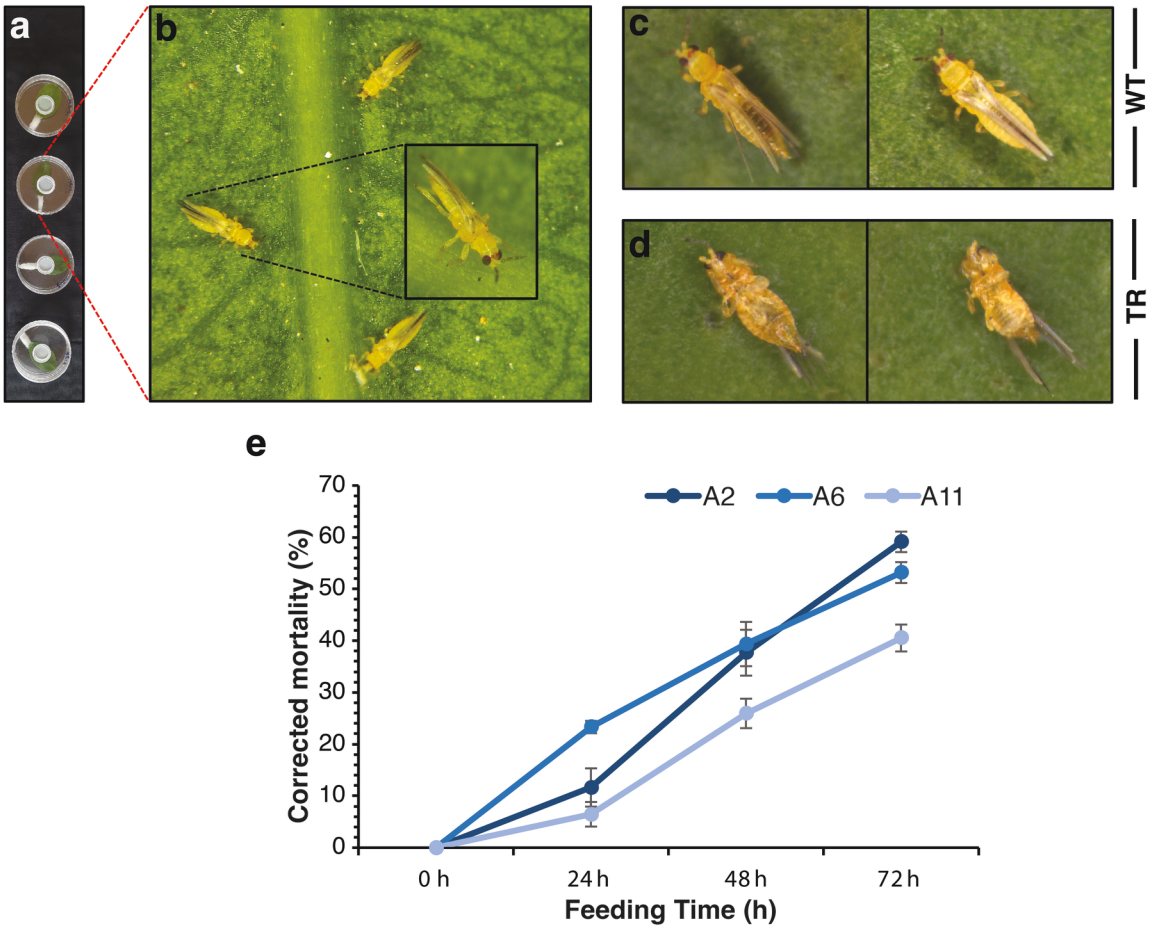

Manuscript image 6.jpg

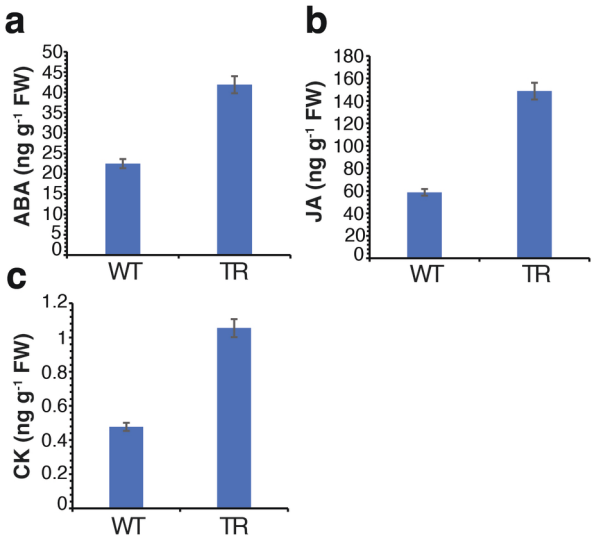

Manuscript image 7.jpg